

PSU/TURBO 82-1

SEMI-ANNUAL PROGRESS REPORT ON
THREE DIMENSIONAL FLOW FIELD INSIDE COMPRESSOR
ROTOR, INCLUDING BLADE BOUNDARY LAYERS

M. POUAGARE, J. M. GALMES, B. LAKSHMINARAYANA,
AND K. N. SACHIDANANDA MURTHY

NASA GRANT Nsg 3266
NATIONAL AERONAUTICS & SPACE ADMINISTRATION
LEWIS RESEARCH CENTER



(NASA-CR-168410) THREE DIMENSIONAL FLOW
FIELD INSIDE COMPRESSOR ROTOR, INCLUDING
BLADE BOUNDARY LAYERS Semiannual Progress
Report (Pennsylvania State Univ.) 87 p
HC A05/MF A01

N82-17175

Unclas
11409

CSCI 21E G3/07

TURBOMACHINERY LABORATORY
DEPARTMENT OF AEROSPACE ENGINEERING
THE PENNSYLVANIA STATE UNIVERSITY
UNIVERSITY PARK, PA 16802

JANUARY 1982

Semi-Annual Progress Report

on

**THREE DIMENSIONAL FLOW FIELD INSIDE COMPRESSOR ROTOR
PASSAGES, INCLUDING BLADE BOUNDARY LAYERS**

**M. Pouagare, J. M. Galmes, B. Lakshminarayana,
and K. N. Sachidananda Murthy**

to

NASA Lewis Research Center

Project Monitor: Dr. P. Sockol

Turbomachinery Laboratory

Department of Aerospace Engineering

The Pennsylvania State University

University Park, PA 16802

January 1982

PREFACE

The progress of research on "Three Dimensional Flow Field Inside a Compressor Rotor Blade Passage, Including Blade Boundary Layers" (NASA Grant NSG 3266) for the six-month period ending December 31, 1981, is briefly reported here. Dr. J. M. Galmas, Research Associate in Aerospace Engineering, has the responsibility for turbulence modelling. Mr. Pouagare, a doctoral candidate, has assumed responsibility for the development of the computer program to predict the blade boundary layer. The measurements reported were carried out by M. Pouagare and K. N. Sachidananda Murthy.

B. Lakshminarayana
Principal Investigator

TABLE OF CONTENTS

	<u>Page</u>
NOMENCLATURE	iv
1. NUMERICAL ANALYSIS OF BLADE AND HUB WALL BOUNDARY LAYERS . . .	1
Introduction	1
Momentum Equations	2
Numerical Solution of the Three Momentum Equations	4
Pressure Correction Equations	6
Status of the Computer Program	9
2. TURBULENCE MODELLING FOR BOTH HIGH AND LOW REYNOLDS NUMBER FLOW SUBJECTED TO ROTATION	10
Introduction	10
Turbulence Equations	13
Qualitative Analysis of k and ϵ Equations	16
k - ϵ Model for High Reynolds Number Flows	19
k - ϵ Model for Low Reynolds Number Flows	22
Eddy Viscosity Law	27
Conclusions	28
3. MEASUREMENTS OF THREE DIMENSIONAL FLOW FIELD INSIDE A COMPRESSOR ROTOR PASSAGE	30
Experimental Program	30
Typical Results	30
4. PAPERS, THESES, AND REPORTS PUBLISHED DURING JULY 1981 - DECEMBER 1981	33
REFERENCES	34
APPENDIX 1 Transformed Momentum Equations and Jacobian Matrices .	39
APPENDIX 2 Literature Survey on the Effects of Curvature and Rotation on Turbulence Structure	48
FIGURES	61

NOMENCLATURE

a_1, a_2, A, B	constants
$C_\mu, C_{\epsilon_1}, C_{\epsilon_2}, C_{\epsilon_3}$	modeling constants
$F_\epsilon(R_T, R_{1c})$	damping function for low Reynolds number flows
g_{ik}	metric tensor
i, j, k	indices in the ξ, n, R coordinates, respectively
J	Jacobian of the transformation
$\bar{k} = \frac{1}{2} g^{ik} \overline{u_i u_k}$	turbulent kinetic energy
l	length scale
p	pressure
\bar{p}	mean pressure
p'	fluctuating pressure
PS	pressure surface
P_S	static pressure
P_T	total pressure of the relative flow
P_{TOTAL}	$P_T / \frac{\rho}{2} U_t^2$
P_{STATIC}	$P_S / \frac{\rho}{2} U_t^2$
r, θ, z	cylindrical coordinate system
R	radial distance normalized by the tip radius
Re	Reynolds number
$Re = \frac{u' l}{\nu}$	local Reynolds numbers
$R_T = \frac{k^2}{\nu \epsilon}$	
$R_{1c} = - \frac{\epsilon}{\bar{u}_{i,j}} \frac{\partial^2}{\partial r^2}$	generalized gradient Richardson number
R_r	$\partial R / \partial r$

S	blade spacing
SS	suction surface
S_{ij}	strain tensor
u', u'^i	fluctuating velocity
t	time
\bar{U}^i	mean contravariant velocity
$\overline{u_i u_j}$	Reynolds tensor
U_t	blade tip speed
U, V, W	velocities in radial, tangential, and axial direction, respectively
v	Kolmogorov velocity scale
W	relative velocity
WR	radial velocity, W_r/U_t
WT	relative tangential velocity, W_θ/U_t
WZ	axial velocity, W_z/U_t
x^j, x_j	contravariant and covariant coordinates variables
Y	tangential distance measured from camber line ($y = 0$ on suction side, $Y = S$ on pressure side for the data in the passage for the wake, $Y = 0$ is the center of the wake)
Z	axial distance normalized by the blade chord ($Z = 0$ at the leading edge)
α, β	constants
δ_{ij}	Kronecker tensor
$\epsilon = 2\nu \overline{s'_{ij} s'^{ij}}$	turbulent dissipation rate
ϵ_{ipq}	permutation tensor
η	Kolmogorov length scale
η_z	$\partial\eta/\partial z$
η_θ	$\partial\eta/r\partial\theta$

μ	molecular viscosity
μ_T	turbulent viscosity
ξ, η, R	transformed coordinates in the streamwise, normal, and radial directions, respectively
ξ_z	$\partial \xi / \partial z$
ξ_θ	$\partial \xi / r \partial \theta$
ρ	density
$\sigma_k, \sigma_\epsilon$	modeling constants
Ω	angular velocity
Ω^P	contravariant component of angular velocity

Subscripts

i, j, k, l, m, n	indices
(p)	value at the wall
r	radial component
S	static
T	total
z	axial component
θ	tangential component

1. NUMERICAL ANALYSIS OF BLADE AND HUB WALL BOUNDARY LAYERS

Introduction

The flow in a turbomachinery blade passage has a predominant flow direction. The viscous diffusion in the streamwise direction is usually small and the elliptic influence is transmitted upstream through the pressure field. So the streamwise diffusion terms in the Navier-Stokes equations can be neglected in comparison to the diffusion in the radial and tangential directions. Starting with a guessed pressure field, it is possible to converge on the full elliptic solution by iterating between a parabolic solution and an iteration of the pressure field. The main steps of the calculation are given below. It is assumed that the properties at the streamwise station i are known and solution at the streamwise station $i + 1$ is sought.

1. The three momentum equations are solved simultaneously to get U, V, W .
2. The energy equation and the perfect gas relation are solved to get the temperature T and the density ρ .
3. The streamwise pressure gradient is corrected by the use of mass conservation across the cross-section.
4. The cross-flow velocity components, determined from the momentum equations, are corrected by including in them the irrotational velocity corrections that satisfy the continuity equation. This step requires the solution of a poisson equation for ϕ defined later.
5. A poisson equation is solved to determine the transverse variation of pressure. The equation for the pressure is derived by appropriately differentiating and summing the two transverse momentum equations.

6. Steps 1 to 5 are repeated until convergence is achieved.
7. Turbulence closure equations are solved to get a new value for the effective viscosity.
8. Solution is marched to the next streamwise station. The flow chart of the computer program is shown on the next page.

The Momentum Equations

The Navier-Stokes equations in cylindrical coordinates are transformed into the computational domain neglecting viscous diffusion terms in the direction ξ .

The transformed equations can be written in the form,

$$\frac{\partial E}{\partial \xi} + \frac{\partial F}{\partial \eta} + \frac{\partial G}{\partial R} + C = \frac{1}{Re} \left[\frac{\partial P}{\partial R} + \frac{\partial Q}{\partial \eta} + S \right] \quad (1)$$

The derivation of this equation is given in Appendix 1.

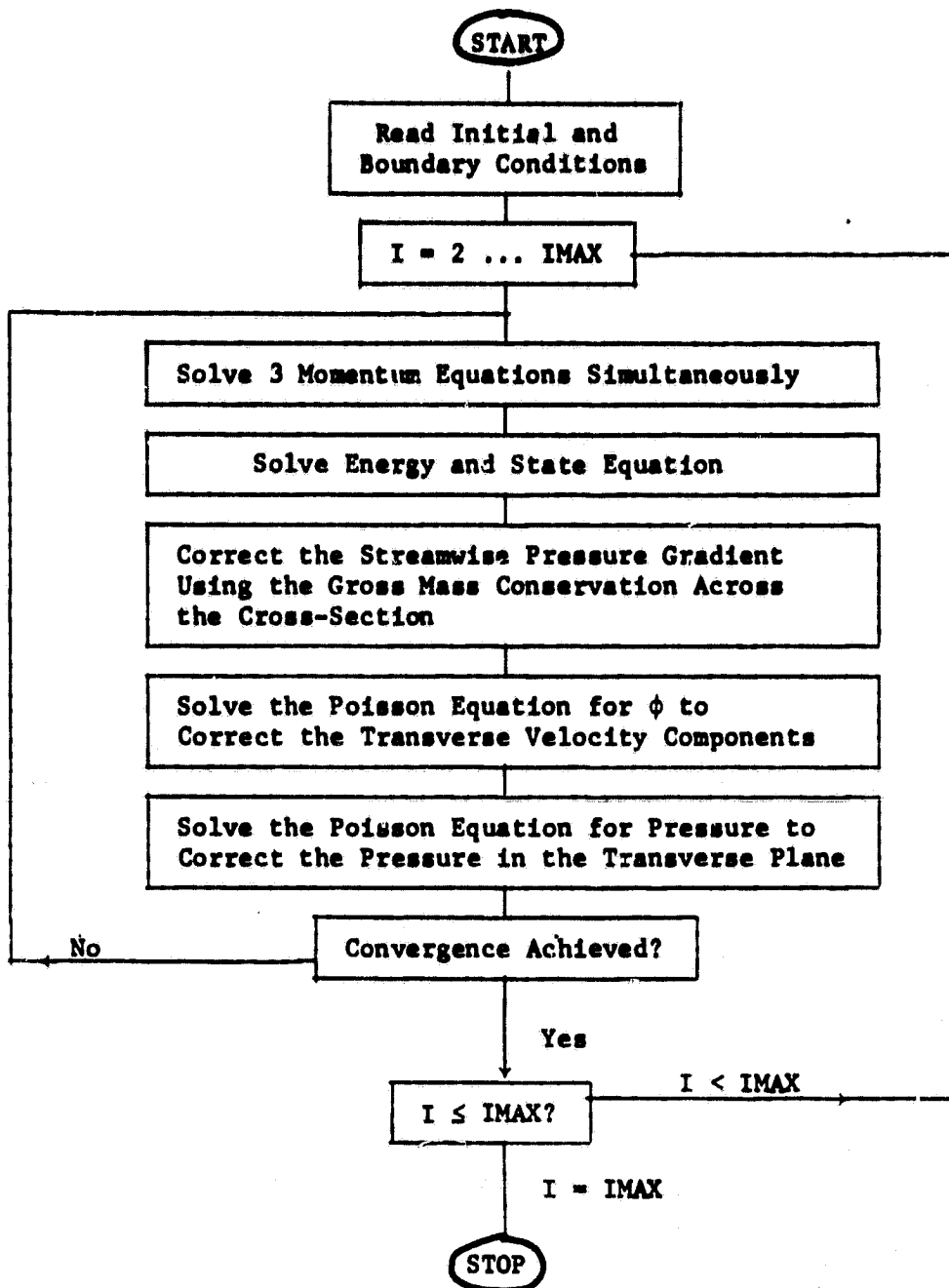
The column vector of unknowns is $g = \begin{bmatrix} U \\ V \\ W \end{bmatrix}$

The column vectors E, F, G, C, P, Q, S are given by

$$E = \frac{1}{J} \begin{bmatrix} \xi_z \rho U^2 + \xi_\theta \rho UV + \xi_z p \\ \xi_z \rho UV + \xi_\theta \rho V^2 + \xi_\theta p \\ \xi_z \rho UW + \xi_\theta \rho VW \end{bmatrix}$$

$$F = \frac{1}{J} \begin{bmatrix} \eta_z \rho U^2 + \eta_\theta \rho UV + \eta_z p \\ \eta_z \rho UV + \eta_\theta \rho V^2 + \eta_\theta p \\ \eta_z \rho UW + \eta_\theta \rho VW \end{bmatrix}$$

$$G = \frac{R}{J} \begin{bmatrix} \rho UW \\ \rho VW \\ \rho W^2 + p \end{bmatrix}$$



Flow Chart for the Computer Program

$$C = \begin{bmatrix} \rho UW/R \\ 2\rho VW/R + 2\rho\Omega W \\ \frac{\rho}{R} [W^2 - V^2] - \rho\Omega^2 R - 2\rho\Omega V \end{bmatrix}$$

$$P = \frac{R_r}{J} \begin{bmatrix} \mu (R_r \frac{\partial U}{\partial R} + \eta_z \frac{\partial W}{\partial \eta}) \\ \mu (\eta_\theta \frac{\partial W}{\partial \eta} + R_r \frac{\partial V}{\partial R} - \frac{V}{R}) \\ \frac{4}{3} \mu R_r \frac{\partial W}{\partial R} - \frac{2\mu}{3} (\eta_\theta \frac{\partial V}{\partial \eta} + \eta_z \frac{\partial U}{\partial \eta} + \frac{W}{R}) \end{bmatrix}$$

$$Q = \begin{bmatrix} \mu \left(\frac{\eta_\theta^2 + \eta_z^2}{J} \right) \frac{\partial U}{\partial \eta} + \frac{\mu}{3} \frac{\eta_z}{J} (\eta_\theta \frac{\partial V}{\partial \eta} + \eta_z \frac{\partial U}{\partial \eta}) - \frac{2}{3} \mu \frac{\eta_z}{J} (R_r \frac{\partial W}{\partial R} + \frac{W}{R}) \\ \mu \left(\frac{\eta_\theta^2 + \eta_z^2}{J} \right) \frac{\partial V}{\partial \eta} + \frac{\mu}{3} \frac{\eta_\theta}{J} (\eta_\theta \frac{\partial V}{\partial \eta} + \eta_z \frac{\partial U}{\partial \eta}) - \frac{2}{3} \mu \frac{\eta_\theta}{J} (R_r \frac{\partial W}{\partial R} + \frac{W}{R}) + 2\mu \frac{\eta_\theta}{J} \frac{W}{R} \\ \mu \left(\frac{\eta_\theta^2 + \eta_z^2}{J} \right) \frac{\partial W}{\partial \eta} + \mu \frac{\eta_\theta}{J} \left[R_r \frac{\partial V}{\partial R} - \frac{V}{R} \right] + \mu \frac{\eta_z}{J} R_r \frac{\partial U}{\partial R} \end{bmatrix}$$

$$S = \begin{bmatrix} \frac{\mu}{R} \left[R_r \frac{\partial U}{\partial R} + \eta_z \frac{\partial W}{\partial \eta} \right] \\ \frac{2\mu}{R} \left[\eta_\theta \frac{\partial W}{\partial \eta} + R_r \frac{\partial V}{\partial R} - \frac{V}{R} \right] \\ \frac{2\mu}{R} \left[R_r \frac{\partial W}{\partial R} - \eta_\theta \frac{\partial V}{\partial \eta} - \frac{W}{R} \right] \end{bmatrix}$$

Numerical Solution of the Three Momentum Equations

The numerical scheme is based on the Linearized Block Implicit Method of Briley and McDonald (1979). Equation 1 is written in the form

$$\frac{\partial H(\mathbf{g})}{\partial \xi} = D(\mathbf{g}) + \hat{S}(\mathbf{g}) \quad (2)$$

where $H(g) = E(g)$

$$D(g) = \frac{1}{R_e} \left[R_r \frac{\partial P}{\partial R} + \frac{\partial Q}{\partial \eta} \right] - \frac{\partial F}{\partial \eta} - \frac{\partial G}{\partial R}$$

$$\hat{S}(g) = S(g) - C(g)$$

The finite difference form of equation (2) is

$$(H^{i+1} - H^i) / \Delta \xi = \beta [D(g) + \hat{S}(g)]^{i+1} + (1 - \beta) [D(g) + \hat{S}(g)]^i$$

where β is the weighting factor.

The linearization is done as follows:

$$H^{i+1} = H^i + \left(\frac{\partial H}{\partial \xi} \right)^i \Delta \xi = H^i + \left(\frac{\partial H}{\partial g} \right)^i \frac{\partial g}{\partial \xi} \Delta \xi = H^i + \left(\frac{\partial H}{\partial g} \right)^i (g^{i+1} - g^i)$$

$$\hat{S}^{i+1} = \hat{S}^i + \left(\frac{\partial \hat{S}}{\partial \xi} \right)^i \Delta \xi = \hat{S}^i + \left(\frac{\partial \hat{S}}{\partial g} \right)^i (g^{i+1} - g^i)$$

$$D^{i+1} = D^i + \left(\frac{\partial D}{\partial \xi} \right)^i \Delta \xi = D^i + \left(\frac{\partial D}{\partial g} \right)^i (g^{i+1} - g^i)$$

The linearized scheme is then given by,

$$\left(\frac{\partial H}{\partial g} \right)^i (g^{i+1} - g^i) / \Delta \xi = D^i + \hat{S}^i + \beta \left[\frac{\partial D}{\partial g} + \frac{\partial \hat{S}}{\partial g} \right] (g^{i+1} - g^i) \quad (3)$$

Defining $A = \left(\frac{\partial H}{\partial g} \right)^i - \beta \Delta \xi \left(\frac{\partial \hat{S}}{\partial g} \right)^i$

$$L = -\beta \frac{\partial D}{\partial g}$$

and

$$\Delta g^{i+1} = g^{i+1} - g^i$$

Equation 3 can be written as

$$(A + \Delta \xi L) \Delta g^{i+1} = \Delta \xi [D + \hat{S}]^i$$

or

$$(A + \Delta \xi (L_\eta + L_R)) \Delta g^{i+1} = \Delta \xi [D + \hat{S}]^i$$

Factorizing the scheme based on the Douglas-Gunn split one gets

$$[A + \Delta\xi L_\eta] \Delta g^* = \Delta\xi [D + S]^{1/2}$$

$$[A + \Delta\xi L_x] \Delta g^{1+1} = A \Delta g^*$$

The Jacobian matrices appearing in equation 3 are given in Appendix 1.

Pressure Correction Equations

The pressure is considered to be composed of three parts.

$$P(\xi, \eta, R) = P_i(\xi, \eta, R) + P_v(\xi) + P_c(\eta, R) \quad (3)$$

P_i is the initial guessed pressure field. $P_v(\xi)$ and $P_c(\eta, R)$ are one- and two-dimensional pressure corrections, respectively.

The velocity components are decomposed as follows

$$\begin{aligned} U &= U^* + U' \\ V &= V^* + V' \\ W &= W^* + W' \end{aligned} \quad (4)$$

U^* , V^* , W^* are the velocity components which are calculated from the momentum equations. U' , V' , W' are the corrections needed for the continuity equation to be satisfied.

The U-momentum equation is written as follows.

$$\begin{aligned}
& \frac{\partial}{\partial \xi} \left(\frac{\xi_z}{J} \rho U^* (U^* + U') + \frac{\xi_\theta}{J} \rho (U^* + U') V^* \right) + \frac{\partial}{\partial \eta} \left(\frac{\eta_z}{J} \rho U^* (U^* + U') + \frac{\eta_\theta}{J} \rho (U^* + U') V^* \right) \\
& + \frac{\partial}{\partial R} \left(\frac{R_r}{J} \rho (U^* + U') W^* \right) + \frac{\rho (U^* + U') W^*}{R} = - \frac{\partial}{\partial \xi} \left(\frac{\xi_z}{J} (P_1 + P_v) \right) \\
& - \frac{\partial}{\partial \eta} \left(\frac{\eta_z}{J} (P_1 + P_c) \right) + \frac{1}{Re} \left\{ \frac{\partial}{\partial R} \left[\frac{R_r}{J} \left[\mu \left(R_r \frac{\partial}{\partial R} (U^* + U') + \eta_z \frac{\partial W^*}{\partial \eta} \right) \right] \right\} \right. \\
& + \frac{\partial}{\partial \eta} \left[\mu \left(\frac{\eta_\theta^2 + \eta_z^2}{J} \right) \frac{\partial}{\partial \eta} (U^* + U') + \frac{\mu}{3} \frac{\eta_z}{J} \left(\eta_\theta \frac{\partial V^*}{\partial \eta} + \eta_z \frac{\partial}{\partial \eta} (U^* + U') \right) \right. \\
& \left. \left. - \frac{2}{3} \frac{\eta_z}{J} \left(R_r \frac{\partial W^*}{\partial R} + \frac{W^*}{R} \right) \right] + \frac{\mu}{R} \left[R_r \frac{\partial (U^* + U')}{\partial R} + \eta_z \frac{\partial W^*}{\partial \eta} \right] \right\}
\end{aligned}$$

The above equation can be rearranged to give,

$$\begin{aligned}
& \frac{\partial}{\partial \xi} \left(\frac{\xi_z}{J} \rho U^* U' + \frac{\xi_\theta}{J} \rho V^* U' \right) + \frac{\partial}{\partial \eta} \left(\frac{\eta_z}{J} \rho U^* U' + \frac{\eta_\theta}{J} \rho V^* U' \right) + \frac{\partial}{\partial R} \left(\frac{R_r}{J} \rho W^* U' \right) + \frac{\rho W^* U'}{R} \\
& = - \frac{\partial}{\partial \xi} \left(\frac{\xi_z}{J} P_v \right) - \frac{\partial}{\partial \eta} \left(\frac{\eta_z}{J} P_c \right) + \frac{1}{Re} \left[\frac{\partial}{\partial R} \left[\frac{R_r^2}{J} \mu \frac{\partial U'}{\partial R} \right] + \frac{\partial}{\partial \eta} \left[\frac{\mu}{J} \left(\eta_\theta^2 + \eta_z^2 \right) \frac{\partial U'}{\partial \eta} + \frac{\mu}{3J} \eta_z^2 \frac{\partial U'}{\partial \eta} \right] \right. \\
& \left. + \frac{\mu}{R} R_r \frac{\partial U'}{\partial R} \right]
\end{aligned}$$

Writing the above equation in finite difference form and dropping the mixed derivatives and the off diagonal terms we get,

$$\begin{aligned}
& \frac{1}{\Delta \xi} \left[\frac{\xi_z}{J} \rho U^* + \frac{\xi_\theta}{J} \rho V^* \right]_{i+1,j,k} U'_{i+1,j,k} + \left(\frac{\rho W^*}{R} \right)_{i+1,j,k} U'_{i+1,j,k} = - \frac{\partial}{\partial \xi} \left(\frac{\xi_z}{J} P_c \right) \\
& - \frac{1}{Re} \left[\left(\frac{R_r^2}{J} \mu \right)_{i+1,j,k+1} + \left(\frac{R_r^2}{J} \mu \right)_{i+1,j,k-1} - 2 \left(\frac{R_r^2}{J} \mu \right)_{i+1,j,k} \right. \\
& + \left[\frac{\mu}{J} \left(\eta_\theta^2 + 1.333 \eta_z^2 \right) \right]_{i+1,j+1,k} + \left[\frac{\mu}{J} \left(\eta_\theta^2 + 1.333 \eta_z^2 \right) \right]_{i+1,j-1,k} \\
& \left. - 2 \left[\frac{\mu}{J} \left(\eta_\theta^2 + 1.333 \eta_z^2 \right) \right]_{i+1,j,k} \right] U'_{i+1,j,k}
\end{aligned}$$

or

$$U' = A \frac{\partial P_c}{\partial \xi} \quad \text{where } A \text{ is a known quantity} \quad (5)$$

Using V momentum equation one gets

$$v' = B \frac{\partial P'}{\partial \xi} \quad \text{where } B \text{ is a known quantity} \quad (6)$$

From continuity equation, we get

$$\iint \frac{\rho}{\eta R \sqrt{1+\eta_x^2}} (U + \eta_x V) dR d\eta = \dot{m} = \text{constant}$$

or

$$\iint \frac{\rho}{\eta R \sqrt{1+\eta_x^2}} (U^* + A \frac{\partial P'}{\partial \xi} + \eta_x V^* + \eta_x B \frac{\partial P'}{\partial \xi}) dR d\eta = \dot{m}$$

$$\frac{\partial P'}{\partial \xi} = \frac{\dot{m} - \iint \frac{\rho}{\eta R \sqrt{1+\eta_x^2}} (U^* + \eta_x V^*) dR d\eta}{\iint \frac{\rho}{\eta R \sqrt{1+\eta_x^2}} (A + \eta_x B) dR d\eta} \quad (7)$$

To correct the cross-flow velocity component the following velocity potential is introduced

$$\frac{\partial \phi}{\partial R} = \frac{R}{J} \rho W' \quad (8)$$

$$\frac{\partial \phi}{\partial \eta} = \frac{\eta_\theta}{J} \rho V' + \frac{\eta_z}{J} \rho U' \quad (9)$$

The continuity equation in the transformed plane becomes

$$\frac{\rho W}{R} + \frac{\partial}{\partial R} \left(\frac{R}{J} \rho W \right) + \frac{\partial}{\partial \xi} \left(\frac{\xi_\theta}{J} \rho V + \frac{\xi_z}{J} \rho U \right) + \frac{\partial}{\partial \eta} \left(\frac{\eta_\theta}{J} \rho V + \frac{\eta_z}{J} \rho U \right) = 0 \quad (10)$$

or

$$\begin{aligned} \frac{\rho}{R} (W^* + W') + \frac{\partial}{\partial R} \left(\frac{R r}{J} \rho (W^* + W') \right) + \frac{\partial}{\partial \xi} \left(\frac{\xi \theta}{J} \rho (V^* + V') + \frac{\xi z}{J} \rho (U^* + U') \right) \\ + \frac{\partial}{\partial \eta} \left(\frac{\eta \theta}{J} \rho (V^* + V') + \frac{\eta z}{J} \rho (U^* + U') \right) = 0 \end{aligned} \quad (11)$$

or

$$\frac{\rho}{R} W' + \frac{\partial}{\partial R} \left(\frac{R r}{J} \rho W' \right) + \frac{\partial}{\partial \xi} \left(\frac{\xi \theta}{J} \rho V' + \frac{\xi z}{J} \rho U' \right) + \frac{\partial}{\partial \eta} \left(\frac{\eta \theta}{J} \rho V' + \frac{\eta z}{J} \rho U' \right) = -\dot{m}^* \quad (12)$$

where \dot{m}^* can be evaluated from U^* , V^* , W^* , ρ . \dot{m}^* should be zero, if continuity is satisfied.

Using equations 5, 6, 8, and 9 in 12 one gets

$$\frac{J}{R} R r \frac{\partial \phi}{\partial R} + \frac{\partial^2 \phi}{\partial R^2} + \frac{\partial^2 \phi}{\partial \eta^2} = -\dot{m}^* - \frac{\partial}{\partial \xi} \left(\frac{\xi \theta}{J} \rho B \frac{\partial P'}{\partial \xi} + \frac{\xi z}{J} \rho A \frac{\partial P'}{\partial \xi} \right) \quad (13)$$

In order to derive the Poisson equation for the pressure, the n-momentum equation is differentiated with respect to η and the R-momentum equation with respect to R . Then they are added together. The result is

$$\frac{\partial}{\partial \eta^2} \left(\frac{\eta \theta}{J} P \right) + \frac{\partial}{\partial R^2} \left(\frac{R r}{J} P \right) = C \quad (14)$$

where C contains known quantities.

Status of the Computer Program

The part of the computer program that solves the three momentum equation has been completed. Coding of the poisson equations is under development.

2. TURBULENCE MODELING OF BOTH HIGH REYNOLDS NUMBER AND LOW REYNOLDS NUMBER FLOWS SUBJECTED TO ROTATION

Introduction

The three dimensional viscous and turbulent effects in turbomachinery are mainly caused by the three dimensional boundary layer on blades and wakes, annulus wall and hub wall boundary layers, shock-boundary layer interaction, and secondary flow. These viscous and turbulence effects play a dominant role in the study of improved design, better efficiency, off design performance, etc.

While appreciable amount of work has been done in understanding the inviscid effects in turbomachinery, there has been no investigation related to the blade boundary layers in compressor rotors. Because of the complicated nature of the problem, compressor, turbine and rotor fan blade boundary layers still continue to be one of the least understood phenomena in turbomachinery. The boundary layers are three dimensional with laminar, transitional, turbulent and separation zones. The flow field is a function of several parameters such as incidence, solidity, blade geometry, hub/tip ratio, camber, radial and chordwise pressure gradients, inlet turbulence, Reynolds number, Rossby number, Mach number, etc.

A knowledge of the boundary layer characteristics, both mean and turbulence properties, is essential in the prediction of flow behavior in these blade passages. The Penn State group, presently involved in the study of the endwall flows, has initiated recently a detailed study, on both the experimental and analytical point of view, of the blade boundary layers. The experimental survey of the flow is in preparation and will be started very soon. The existing and well proven techniques of single hot wire and x-wire are to be used in measuring the development of boundary layers on turbomachinery

rotor blades. Both measurements of mean and turbulent flow field are to be performed.

Analysis of three dimensional boundary layer is equally complex due to the fact that additional effects such as Coriolis and Centrifugal forces change the structure of turbulence, thus invalidating most of the turbulence models that are presently used in computing turbulent boundary layers. In the case of turbomachinery rotor flows, the turbulence is affected mainly by the curvatures of both the blade surface and the streamlines, by the body rotation, and in the case of the boundary layer, by the low Reynolds number effects. All these effects make the flow to be highly non-isotropic. Moreover, as it can be seen in the experimental results of Castro and Bradshaw (1976) and, Johnston, Halleen and Lezius (1972), the curvature and/or the rotation may affect the stability of the boundary layer and an augmentation or suppression of the turbulence may result. With such phenomena occurring, it appears that assumptions based on the well known isotropic eddy viscosity concept should fail badly, as the Reynolds stress tensor is not aligned with the mean strain tensor when additional production or destruction of turbulence are coupled with the production due to the shear.

Most of the present models are valid for non-rotating systems. These include Jones and Launder (1972) for $k-\epsilon$, Launder, Reece, and Rodi (1975) and Lumley and Khajeh-Nouri (1974) for the full Reynolds stress model. The effects of curvature in high Reynolds number flows have not yet been accounted for properly in the turbulence modeling. We may mention the attempt by Gibson and Rodi (1981). As far as the rotation effects are concerned, very few attempts have been made to introduce such effects in the calculation schemes. However, in the available turbulence models, the effect of rotation is not properly modeled in the transport equations of Reynolds stress or the dissipation rate. Moreover, the boundary layers flows are of the low

Reynolds' number type. If we are interested in modeling the turbulence behavior very near the wall, then it is necessary to introduce this effect in the modeling assumptions.

The formulation of the closure problem will vary depending upon the information and accuracy desired. In fact, the calculation procedures for three-dimensional viscous flows require large memory storage and large computer time to solve the three momentum and continuity equations. Moreover, such codes are still in a phase of development and are generally tested only for simple cases (e.g., laminar flows). Hence, the introduction of turbulence models in these codes necessitate careful attention and simple models may permit control of the stability of the numerical scheme. However, in rotating turbulent flows, zero equation models fail to represent even the gross properties, due to the fact that the length and time scales are assumed empirically. The two-equation model is a compromise between a full Reynolds stress model which needs the resolution of seven more transport equations as complicated as the Navier-Stokes equations themselves, and the empirical models. Therefore, as a first step, attempts are being made to include the effect of rotation in the k - ϵ model. Modeling of the rotation effect and the low Reynolds number effect in the turbulence closure equations are described in this report.

A literature survey on both the analytical and the experimental work is given in Appendix 2. Some of the important conclusions of this survey are:

1. Only few calculations are available for the calculation of the three-dimensional boundary layer in rotating frames.
2. No complete Reynolds stress model is available for rotating turbulent flows. Very few attempts have been made to account for the rotation effects

in the $k-\epsilon$ model, but none are really based on a logical analysis. In fact, the most up to date results in modeling are those of Raj (1975) and Hah and Lakshminarayana (1980). The major effort, then, should be given to the analysis of the dissipation rate equation and to the Reynolds stress equations.

3. Detailed measurements providing informations on the effects of both the Rossby and the Richardson number on turbulence are not very numerous. So, every new result would be of great interest, particularly if the rotation effect can be isolated from the other effects.

Turbulence Equations

The turbomachinery boundary layers and wake must be represented in a relative rotating frame of reference, which includes both the curvature and rotation terms, to eliminate the effect of periodic unsteadiness. The transformation of the turbulence equations as well as the momentum equations from a stationary coordinate system to a rotating coordinate system is quite complicated. Moreover, the necessity for the turbulent model to be as general as possible, indicates that the generalized tensor formulation is the most adequate representation of the set of equations. The equations of the mean and turbulent quantities representing an incompressible flow are derived in a rotating frame and are presented in conservative form.

Continuity equation

$$\bar{U}_{,i}^i = 0 \quad u'_{,i}{}^i = 0 \quad (15)$$

Momentum equations

$$(\rho \dot{\bar{U}}_i) + (\rho \bar{U}_i \bar{U}^j)_{,j} + 2\epsilon_{ipq} \rho \Omega^p \bar{U}^q + \rho [(\Omega_j x^j)_{,i} - (\Omega_j \Omega^j) x_i] = -(\bar{p} \delta_i^j + \overline{\rho u'_i u'^j} - P_i^j)_{,j} \quad (16)$$

with $P_1^j = 2\mu S_1^j$ for Newtonian fluid and $S_{1j} = \frac{1}{2}(\bar{U}_{1,j} + \bar{U}_{j,1})$.

Reynolds stress equations

$$\begin{aligned}
 (\rho \overline{u'_j u'_k}) + (\rho \overline{u'_1 u'_k} \bar{U}^j)_{,j} &= -(\overline{p' u'_1} \delta_k^j + \overline{p' u'_k} \delta_1^j + \rho \overline{u'_1 u'_k u'^j} - \overline{u'_1 p^j} - \overline{u'_k p^j})_{,j} \\
 &+ \overline{p' u'_{1,j}} \delta_k^j + \overline{p' u'_{k,j}} \delta_1^j - \rho \overline{u'_1 u'^j} \bar{U}_{k,j} - \rho \overline{u'_k u'^j} \bar{U}_{1,j} \\
 &- \overline{p^j_{k'1,j}} - \overline{p^j_{1'k,j}} - 2\rho \Omega^P (\epsilon_{1pq} \overline{u'_k u'^q} + \epsilon_{kpq} \overline{u'_1 u'^q})
 \end{aligned} \tag{17}$$

Kinetic energy equation

$$\begin{aligned}
 \frac{1}{2} g^{ik} \overline{u'_i u'_k} &= \bar{k} \\
 (\rho \dot{\bar{k}}) + (\rho \bar{k} \bar{U}^j)_{,j} &= -(\overline{p' u'_1} \delta^{1j} + \rho \overline{ku'^j} - \overline{u'_1 p^{1j}})_{,j} - \rho \overline{u'^1 u'^j} \bar{U}_{1,j} - \overline{p^{1j} u'_{1,j}}
 \end{aligned} \tag{18}$$

where $-\rho \overline{u'^1 u'^j} \bar{U}_{1,j}$ = production and $\overline{p^{1j} u'_{1,j}} = \rho \epsilon = 2\mu S'_{1j} S'^{1j}$

Dissipation equation

$$\begin{aligned}
 (\rho \dot{\epsilon}) + (\rho \epsilon \bar{U}^j)_{,j} &= -4\mu (\overline{S'_{1k} u'^j} S'^{1k})_{,j} - (\rho \epsilon u'^j)_{,j} + g^{nj} \epsilon_{,nj} - 4\mu \bar{U}^j_{,k} \overline{S'^{1k} u'_{1,j}} \\
 &- 4\mu \bar{U}_{1,j} \overline{S'^{1k} u'_{k,j}} - 4\mu \overline{S'^{1k} u'_{1,j} u'_{k,j}} - 4\mu v g^{nj} \overline{S'^{1k} S'_{ik,n}} \\
 &- 4\nu \overline{S'^{1k} p'_{,ik}} - 8\mu \epsilon_{ipq} \Omega^P \overline{S'^{1k} u'_{k,q}}
 \end{aligned} \tag{19}$$

The curvature terms are implicitly included in equations 15 through 19. The rotation effect appears both explicitly and implicitly. We are now focusing our analysis on the rotation effect principally.

In the momentum equation, the rotation appears through the Coriolis and Centrifugal forces, but it also affects implicitly the results through the Reynolds stresses. In fact, looking at equation 17, these Reynolds stresses

are explicitly affected by the Coriolis forces, but are also implicitly affected by the rotation through the triple velocity correlations, the pressure velocity correlations, the pressure strain correlation, the production by the stresses themselves, and the dissipation.

Following these remarks it is evident that a full Reynolds stress model should give better results than the models based on an isotropic eddy viscosity hypothesis, particularly in three-dimensional flows.

However, the difficulty to handle solution procedures for three dimensional turbulent flows and the particular problem of modeling the dissipation equation lead us, in a first step, to direct our efforts in developing a $k-\epsilon$ model for both high and low Reynolds number flows. This model necessitates the resolution of two transport equations for k and ϵ , and the Reynolds stresses are related to the mean strain through an eddy viscosity. The present $k-\epsilon$ model cannot account for the anisotropy of the turbulence which exists in the boundary layer around a blade. A modification to the relation giving the eddy viscosity is presently under development, in order to include the effects of the rotation.

The rotation also appears explicitly in the equation for the dissipation rate ϵ . It seems [Hanjalic and Launder (1978)] that some of the major problems in calculations come from the modeled equation for the dissipation rate ϵ . Hence, there is a need for better analysis of this equation. Following Tennekes and Lumley (1972), we may develop a qualitative analysis of the equations k and ϵ in order to provide the magnitude of each term and then to derive a model for high Reynolds number and low Reynolds number flows.

Qualitative Analysis of k and ϵ Equations

Equation 18 represents the evolution of the kinetic energy k . It is interesting to note that the rotation term vanishes identically, and this equation is independent of the coordinate system. It is clear, however, that even though the Coriolis forces have no direct effects in this equation, the rotation affects the kinetic energy principally through the production by the mean strains and also through the dissipation term. The production term depends on how the Reynolds stresses are represented and the dissipation term is described by equation 19, which is the exact form of the equation of evolution for the dissipation rate. Different authors have pointed out the difficulty in solving this equation, and one of the most suitable methods to simplify the equation is to use the high Reynolds number approximation. With this assumption, terms which are dominant at low Reynolds number are eliminated. At this point, we may note that equation 19 is not independent of the transformation from a non-inertial frame of reference to a rotating frame.

In Tennekes and Lumley (1972), it is shown how orders of magnitude may be assigned to various correlations appearing in these equations. Instantaneous quantities appearing in the correlations are of two types, belonging either to the energy containing range of eddies, or to the dissipation range. The former has characteristic frequency u'/ℓ (where u' is a fluctuating velocity scale, while ℓ is a length scale of the gross structures). The dissipation rate is of order u'^3/ℓ . The latter has characteristic frequency v/η (where v and η stand for the Kolmogorov velocity and length scales), with $v/\eta \sim Re^{1/2} u'/\ell$ (with $Re = u'\ell/\nu$). The correlation coefficient between two quantities from the same range may usually be taken as unity, but the coefficient between two quantities from different range is of order of the time scale

ratio $\eta/\nu/\ell/u' \sim Re^{-1/2}$. In addition, we may make use of the more familiar fact that derivatives which are external to correlations correspond to scales in the energy containing range, while derivatives within the correlation correspond to dissipation scales. We wish to apply this sort of reasoning to the equations for the kinetic energy k and its dissipation rate ϵ . Applied to the dissipation equation it is particularly useful, because the dynamics of these quantities is dominated by the small scales, and interacts only weakly with the energy containing eddies. Proceeding in this way, we may provide an order of magnitude for each term of equations 18 and 19.

Kinetic Energy Equation (equation 18)

The convective terms $(\rho \dot{\bar{k}}) + (\rho \bar{k} \bar{u}^j)_{,j}$ are of the same order as $\rho \frac{(u')^3}{\ell}$

The production term $(-\rho \overline{u'^1 u'^j} \bar{u}_{1,j})$ is of order $\rho \frac{(u')^3}{\ell}$

The dissipation term $(-\rho \epsilon)$ is of order $\rho \frac{(u')^3}{\ell}$

In the "diffusion" term $-(\overline{p' u'^1} \delta^{1j} + \rho \overline{k u'^j} - \overline{u'^1 p'^j})_{,j}$, the two first terms are of order $\rho \frac{(u')^3}{\ell}$, while the last one, representing the diffusion by the molecular processes, is of order $\rho \frac{(u')^3}{\ell} Re^{-1}$ and is negligible for high Reynolds number flows.

Dissipation Equation (equation 19)

The convective terms $(\rho \dot{\bar{\epsilon}}) + (\rho \bar{\epsilon} \bar{u}^j)_{,j}$ are of the same order $-\rho \frac{(u')^4}{\ell^2}$.

The terms involving derivatives of mean strain $-4\mu \overline{S'^1_k u'^j} \bar{S}^1_k$ is of the order $\rho \frac{(u')^4}{\ell^2} Re^{-1}$.

The terms involving mean derivatives and rotation

$$-4\mu \bar{u}^j_{,k} \overline{S'^1_k u'^j} - 4\mu \overline{S'^1_k u'^j}_{,k} (\bar{u}_{1,j} + 2\epsilon_{ipj} \Omega^p)$$

Following Lumley (1970), we may model the quantities $\overline{s'^{1k}_{u'_{i,j}}}$ and $\overline{s'^{1k}_{u'_{i,k}}}$ and then we write

$$\overline{s'^{1k}_{u'_{i,j}}} \approx \frac{\epsilon}{3\nu} \left(\delta_j^k + \alpha \sqrt{\frac{\nu}{\epsilon}} s_j^k \right)$$

$$\overline{s'^{1k}_{u'_{i,k}}} \approx \frac{\epsilon}{3\nu} \left(\delta^{1j} + \beta \sqrt{\frac{\nu}{\epsilon}} s^{1j} \right)$$

and since the mean flow is considered incompressible the only terms which contribute are the second terms in the last two relations. Therefore, the first term involving mean derivatives is of the order $\rho \frac{(u')^4}{\rho^2} Re^{-1/2}$ and the second term is of order $\rho \frac{(u')^4}{\rho^2} Re^{-1/2} \left(1 + 2 \frac{\Omega \rho}{u'} \right)$.

The terms involving the triple correlation between the fluctuating derivatives $-4\mu \overline{s'^{1k}_{u'_{i,j}} u'_{i,k}}$. Following once again Lumley (1970) it is of the order

$$\mu \left(\frac{\epsilon}{\nu} \right)^{3/2} \left(B + \mathcal{O} \left(S_{1k} S^{1k} \frac{\nu}{\epsilon} \right) \right)$$

Therefore it is of order $\rho \frac{(u')^4}{\rho^2} Re^{-1/2} (B + Re^{-1})$.

The terms involving the correlation with pressure fluctuations

$$-4\nu \overline{s'^{1k}_{p'_{i,k}}}$$

We may write a poisson equation for this term and then the solution of the equation is as follows: [Chou (1945)]

$$\nu \overline{s'^{1k}_{p'_{i,k}}} = \frac{\mu}{2\pi} \iiint \left[\overline{u^m_{(1),n} (u^n_{(1)} s'^{1k})} \right]_{(1),ki} \frac{dv_{(1)}}{X}$$

$$+ \frac{\mu}{2\pi} \iiint \left[\overline{u^m_{(1)} u^n_{(1)} s'^{1k}} \right]_{(1),mki} \frac{dv_{(1)}}{X}$$

$$+ \frac{\nu}{4\pi} \iint \left[\frac{1}{X} \frac{\partial (P'_{(1),k} s'^{1k})}{\partial n_{(1)}} - \overline{P'_{(1),k} s'^{1k}} \frac{\partial 1/X}{\partial n_{(1)}} \right] dS_{(1)}$$

This solution introduces higher level of correlation and then, at this level of closure assumption we may neglect this term.

The terms involving the correlation between the derivatives of the fluctuating strain

$$-4\mu\nu g^{nj} \overline{s'_{jk} s'_{ik,n}} \sim \left(\frac{\epsilon}{\nu}\right)^{3/2} \left(\Lambda + C(s'_{ik} s'_{ik} \frac{\nu}{\epsilon})\right)$$

Therefore it is of order

$$\rho \frac{(u')^4}{l^2} Re^{1/2} (\Lambda + Re^{-1})$$

The "diffusion" terms $-(\rho\epsilon U'^j)_{,j} + g^{nj} \mu \epsilon_{,nj}$. The first term is of order $\rho \frac{(u')^4}{l^2}$ while the last one is of order $\rho \frac{(u')^4}{l^2} Re^{-1}$.

This order of magnitude analysis is summarized in Table 1.

k-ε Model for High Reynolds Number Flows

High Reynolds number flows occur generally far from walls, in that case the viscous diffusion may be neglected in equation 18, then only the diffusion term $(\rho k u'^j + p' u'^j)_{,j}$ needs to be modeled. For this term we follow the proposition of Jones-Launder and we write (in generalized tensor notation)

$$(\rho k u'^j + p' u'^j)_{,j} = -g^{lj} \left[\frac{\mu_T}{\sigma_k} \bar{k}, l \right]_{,j}$$

The production term is defined through the law of eddy viscosity.

In regard to the dissipation equation, we may neglect all the terms of order of magnitude less than $\rho \frac{(u')^4}{l^2}$; therefore, the only terms left are the convective terms, the "turbulent diffusion" and the production and dissipation by the correlations of fluctuating derivatives (Table 1). These two terms have been derived by Lumley and Khajeh-Nouri (1974). At this point

Table 1. Order of Magnitude of Terms in the Dissipation Equation

Physical Nature	Term	Order of Magnitude
Convection	$(\rho \bar{\epsilon}) + (\rho \epsilon \bar{u}^j),_j$	$\rho \frac{(u')^4}{l^2} \times 1$
Diffusion	$g^{nj} \mu \epsilon_{,nj} - (\rho \epsilon u',j),_j$	$\rho \frac{(u')^4}{l^2} \times (1 - Re^{-1})$
Production by Mean Strain Derivatives	$-4\mu \overline{(S'_{ik} u',j S'_{,j} ik)}$	$\rho \frac{(u')^4}{l^2} \times Re^{-1}$
Production by Mean Strain and Rotation	$-4\mu \bar{u}^j_k \overline{S'_{ik} u',j} - 4\mu \bar{u}^j_{i,j} \overline{S'_{ik} u',k} - 8\mu \epsilon_{ipq} \Omega^p \overline{S'_{ik} u',k}$	$\rho \frac{(u')^4}{l^2} \times Re^{-1/2} (1 + \frac{\Omega^2}{u'^2})$
Production by Fluctuating Strains	$-\overline{S'_{ik} u',j u',j} u',k$	$\rho \frac{(u')^4}{l^2} \times Re^{1/2} (1 + Re^{-1})$
Decay Due to Fluctuating Strain	$-4\mu \nu g^{nj} \overline{S'_{ik} S'_{,j} ik},n$	$\rho \frac{(u')^4}{l^2} \times Re^{1/2} (1 + Re^{-1})$

of modeling, assumptions to get these two terms are widely based on physical and dimensional analysis. In fact, for high Reynolds number flows, the dissipation processes occur almost only at high wave numbers (e.g., the smallest structures); therefore, an isotropy hypothesis may represent the small structures quite well. Moreover, looking at the kinetic energy spectrum we may assume that three zones are defined, the production zone (low wave numbers), the inertial zone, and the dissipative zone (high wave numbers). By this way, a time scale based upon the time that the gross structures transfer their energy to the dissipative structures may be defined. This time scale is of the order of k/ϵ . So, the processes are simplified, and the ϵ equation may be written in the transport form where the sources and dissipation terms are related to those existing in the k equation, by the time scale. Then following Lumley and Khajeh-Nouri (1974), the equation 19 reduces to

$$(\dot{\rho\epsilon}) + (\rho\epsilon\bar{U}^j),_j + (\overline{\rho\epsilon u^i u^j}),_j = C_{\epsilon_1} \frac{\epsilon P}{k} - C_{\epsilon_2} \rho \frac{\epsilon^2}{k}$$

The "diffusion term" may be approximated by a gradient formulation (Jones-Launder). Then with the formulation for the eddy viscosity, the model is complete; the constants σ_k , σ_ϵ , C_{ϵ_1} , C_{ϵ_2} appearing in equation 20 are those found by Jones and Launder (1972)

$$(\dot{\rho\bar{k}}) + (\rho\bar{k}\bar{U}^j),_j = g^{lj} \left[\frac{\mu_T}{\sigma_k} \bar{k},_l \right],_j + P - \rho\epsilon$$

$$(\dot{\rho\epsilon}) + (\rho\epsilon\bar{U}^j),_j = g^{lj} \left[\frac{\mu_T}{\sigma_\epsilon} \epsilon,_l \right],_j + C_{\epsilon_1} \frac{\epsilon}{k} P - C_{\epsilon_2} \frac{\epsilon^2}{\bar{k}} \quad (20)$$

The formulation for the eddy viscosity proposed by Jones-Launder is given by,

$$\mu_T = C_\mu \rho \frac{k^2}{\epsilon}$$

This formula assumes a local equilibrium between the production and the dissipation of turbulence. But in the case of a rotation, the production and the dissipation evolve differently because of the differences in the range of wave number the two processes are occurring. As the production is principally located in the low wave number zone, the effect of the rotation should be more important on the production than on the dissipation which can be seen as nearly isotropic. Therefore, the relation giving the eddy viscosity should be corrected in the case of a rotation. This is being presently carried out.

We may remark at this point that no direct effect of rotation appears in the dissipation equation derived for high Reynolds number flows. That can be related to the weak anisotropy of the dissipation in that case. The analysis given above has been carried out earlier, except for its representation in a generalized tensor form.

k-ε Model for Low Reynolds Number Flows

First of all, we may want to define what we call a "low Reynolds number flow". If we are interested on the statistical properties of the turbulence, it is useful to define local parameters, such as local Reynolds number based on the turbulent quantities, Richardson numbers, etc. The Reynolds number which is interesting to characterize the turbulence behavior is based on the kinetic energy and its dissipation rate and is written as follows:

$$R_T = \frac{k^2}{\nu \epsilon} \sim Re$$

The fact that a flow will be of the high or low Reynolds number type will depend on the value of R_T .

For low Reynolds number flows the viscous diffusion may not be neglected, moreover very near a wall the dissipation is not isotropic. Many of the terms we were neglecting may be important very near a wall. Therefore we must go back to equations 18 and 19 and analyze the terms which were neglected before.

Equation for the Turbulent Kinetic Energy k

The production and turbulent diffusion terms are modeled similar to the high Reynolds number and the effect of low Reynolds number will appear through the eddy viscosity. The only term which needs to be modeled is the viscous term $(u'_i p'^{ij})_{,j}$. This term is equal to $g^{lj} [\mu \bar{k}_{,l} + \mu (u'_i u'_l)_{,i}]_{,j}$

Generally the value of the dissipation at the wall is different from zero. Following the argument of Jones and Launder (1972), it is useful to make the dissipation ϵ equal to zero at the wall for improvement in calculation. It is necessary, then, to know the value of the dissipation at the wall. We may write the kinetic energy equation at the wall, then equation 18 becomes

$$(\rho \epsilon)_{(p)} = g^{lj} \left[\left(\mu + \frac{\mu_T}{\sigma_k} \right) \bar{k}_{,l} + \mu (u'_i u'_l)_{,i} \right]_{,j(p)}$$

And introducing the following hypothesis:

1. $\mu_T = 0$ at the wall

2. If y is the normal direction to the wall, we may write

$$u' = a(t)y; v' = b(t)y^2; w' = c(t)y. \quad \text{Therefore very near the wall } (y^+ \leq 8)$$

the kinetic energy is $k = (a^2 + c^2)/2 * y^2$; then the first derivative of k is zero at the wall, while the second derivative is a constant.

3. $\mu_T = C_{\mu} F_{\mu} \rho \frac{k^2}{\epsilon}$ with $\epsilon \sim k^{3/2}/\ell$ and ℓ is a mixing length then $\mu_T \sim y^2$ and the first derivative of μ_T should be zero, while the second derivative should be a constant. Then $(\rho \epsilon)_{(p)} = g^{lj} \left(\frac{5}{3} \mu \bar{k}_{,lj} - \mu v_{T,ij} S_{lj}^i \right)_{(p)}$.

Moreover, if we use the correction function F_μ for the sublayer in the relation for μ_T , it appears that we may neglect the second term. Therefore

$$(\rho\varepsilon)_{(p)} \approx g^{lj} \frac{5}{3} \mu \bar{k}_{,lj}(p) \text{ which is a constant.}$$

This can be written, following Jones-Launder (1972), as

$$(\rho\varepsilon)_{(p)} = \frac{10}{3} \mu g^{lj} k_{,l}^{1/2} k_{,j}^{1/2}$$

Which can be seen as a generalization to the formulation proposed by Jones and Launder for a two dimensional boundary layer.

$$(\rho\varepsilon)_{(p)} = 2\mu \left(\frac{\partial k}{\partial y} \right)^2$$

The kinetic energy equation reduces then to

$$(\rho\bar{k})_{,j} + (\rho\bar{k}\bar{u}^j)_{,j} = g^{lj} \left(\left(\mu + \frac{\mu_T}{\sigma_k} \right) \bar{k}_{,lj} \right)_{,j} + P - \rho\varepsilon - \frac{10}{3} g^{lj} \mu \bar{k}_{,l}^{1/2} \bar{k}_{,j}^{1/2} \quad (21)$$

Equation for Dissipation Rate

The effect of rotation may be important in low Reynolds number flows (near a wall) unlike the high Reynolds number case (particularly in the case of turbomachines). This effect must be modeled in the equation. But this term is not the only one to be retained in the equation, some other terms which are related to the anisotropy of the dissipation at low Reynolds numbers are of the same importance.

Two kinds of terms may be discerned, which are important at low Reynolds numbers (see Table 1 and equation 19).

1. Terms of Order $R_T^{-1/2}$

These terms come from the interaction of the dissipation with the mean gradients and with the rotation velocity. They also arise from the terms representing the production of velocity gradients by stretching by fluctuating strain rate and representing the destruction of these gradients by viscosity on the other hand.

The terms related to mean quantities are

$$-4\mu[\bar{u}_{,k}^j \overline{s_{,i}^{ik} u_{,j}'} + (\bar{u}_{1,j} + 2\varepsilon_{ipj} \Omega^P) \overline{s_{,i}^{ik} u_{,k}'}]$$

Then following Lumley (1970) this term can be reduced to:

$$-\frac{4}{3} \mu \sqrt{\frac{\varepsilon}{\nu}} \left[\alpha \bar{u}_{,k}^j s_{,j}^k + \beta \left(1 + 2 \frac{\varepsilon_{ipj} \Omega^P}{\bar{u}_{1,j}} \right) \bar{u}_{1,j} s^{ij} \right]$$

In the case of a turbomachinery with $\Omega = (0, 0, \Omega_3)$, the coefficient

$\left(1 + 2 \frac{\varepsilon_{ipj} \Omega^P}{\bar{u}_{1,j}} \right)$ may be simplified. In fact this term appears to be important only very near a wall. Therefore, in this region the boundary layer approximations are valid and the coefficient may be approximated using the only velocity gradients which are important. We may, then define a gradient Richardson number as follows:

$$R_{ic} = -2 \frac{\varepsilon_{ipj} \Omega^P}{\bar{u}_{1,j}}$$

Hence,

$$1 + 2 \frac{\varepsilon_{ipj} \Omega^P}{\bar{u}_{1,j}} = 1 - R_{ic}$$

If we assume that a relation of the gradient type exists between the Reynolds stress tensor and the strain tensor and that the energy spectrum is not different from an equilibrium one, then we may assume that this term is proportional to the production, then the terms related to mean quantities can be proportional to

$$\frac{4}{3} \frac{\varepsilon}{k} P F_1 (R_T, R_{ic})$$

The terms related to fluctuating strain rate are

$$-4\mu \overline{s'_{i,j}{}^{ik} u'_{i,j}{}^{j} u'_{i,k}{}^{j}} - 4\mu \nu g^{nj} \overline{s'_{i,j}{}^{ik} s'_{ik,n}}$$

Following Lumley (1970) we approximate these two terms as follows:

$$\overline{s'_{i,j}{}^{ik} u'_{i,j}{}^{j} u'_{i,k}{}^{j}} \approx \left(\frac{\epsilon}{\nu}\right)^{3/2} (B + a_1 S_{ik} S_{ik}^{ik} \nu/\epsilon)$$

$$g^{nj} \overline{s'_{i,j}{}^{ik} s'_{ik,n}} \approx \left(\frac{\epsilon}{\nu}\right)^{3/2} (A + a_2 S_{ik} S_{ik}^{ik} \nu/\epsilon)$$

Then the part which is of order $R_T^{-1/2}$ may be approximated by:

$$4 \frac{\epsilon}{k} P F_2 (R_T)$$

So the total contribution of terms of order $R_T^{-1/2}$ may be reduced to:

$$\frac{\epsilon}{k} P F(R_T, R_{ic})$$

where the function F must be established.

2. Terms of Order R_T^{-1}

There are two terms of this kind, the first one represents "exactly" the diffusion processes by molecular viscosity and does not need to be modeled; the second term is $-4\mu \overline{s'_{ik} u'_{i,j}{}^{j} s'_{i,j}{}^{ik}}$. We may note that the correlation between s'_{ik} and $u'_{i,j}{}^{j}$ should be weak because each term belongs to a different range of wave number. A first approximation then, is to consider the term $\overline{s'_{ik} u'_{i,j}{}^{j}}$ as a flux of s'_{ik} by $u'_{i,j}{}^{j}$ and to introduce the gross hypothesis that this flux is related to the gradient of the mean strain and then:

$$-4\mu \overline{s'_{ik} u'_{i,j}{}^{j} s'_{i,j}{}^{ik}} \approx 4\mu \nu_T C'_{\epsilon_3} g^{lj} (s_{ik,l} s'_{i,j}{}^{ik})$$

However this term should be of little importance in the major part of the boundary layer.

It is remarkable that this term can be considered as a generalization of a term proposed by Jones and Launder (1972) for the calculation of a two dimensional boundary layer. Therefore, the dissipation equation reduces to:

$$\begin{aligned}
 (\rho \epsilon) + (\rho \epsilon \bar{U}^j)_{,j} = & g^{lj} \left[\left(\mu + \frac{\mu_T}{\sigma_\epsilon} \right) \epsilon_{,l} \right]_{,j} + C_{\epsilon_1} F_\epsilon (R_T, R_{1c}) \frac{\epsilon}{k} P \\
 & + C_{\epsilon_2} \rho \frac{\epsilon^2}{k} + C_{\epsilon_3} \mu \nu_T g^{lj} (S_{ik,l} S^{ik})_{,j} \quad (22)
 \end{aligned}$$

The constants σ_ϵ , C_{ϵ_1} , C_{ϵ_2} are the same as the ones for the high Reynolds number case. The constant C_{ϵ_3} reduces to the value 2, in the case of a two dimensional boundary layer [see Jones-Launder (1972)]. Then, the damping function F_ϵ must be established. According to the analysis given above F_ϵ should be a linear function of the Richardson number and an exponential function of the Reynolds number. Then the form of F_ϵ should be:

$$F_\epsilon (R_T, R_{1c}) = 1 - f(R_T) (1 - \alpha R_{1c})$$

Eddy Viscosity Law

We need a formulation to relate the Reynolds stress tensor to the strain tensor, through an eddy viscosity coefficient. This hypothesis means that [Tennekes-Lumley (1972)] the gross structures get the tendency to be oriented with the principal axis of the strain tensor to extract more energy to the mean field, and that the turbulent structures are approximately convected within the mean velocity direction. Therefore, the main hypothesis to derive the viscosity law assumes that the turbulent viscosity is isotropic. But for three dimensional flows and particularly for boundary layer flows, the velocity vector \vec{U} and $\vec{\nabla U}$ are not aligned in general. Therefore, the

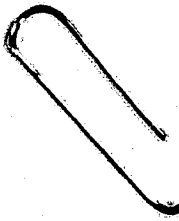
isotropic eddy viscosity is not adapted to predict the behavior of the Reynolds stresses. The best way to avoid this problem would be to solve the complete set of Reynolds stresses equations. However, as first step attempts will be made to derive an expression for eddy viscosity. In fact, in its most general form the eddy viscosity is a fourth order tensor, and for the particular case where only two directions in the flows are of equal importance (that is the case for blade boundary layers) we may introduce two different eddy viscosity coefficients which can take account for the non-isotropy of the flow. This has been done for a mixing length hypothesis by Koosilin and Lockwood (1974). Using this concept, the anisotropy introduced by the rotation could be included in the definition of the viscosity law.

An attempt is presently under development to take account for the effect of the rotation in the eddy viscosity law.

Conclusion

✓ The analysis of the kinetic energy and the dissipation equation has been performed, and some remarks can be made at this time.

Firstly, an order of magnitude analysis of equations 18 and 19 showed that the rotation does not affect the dissipation rate explicitly in high Reynolds number flows. In fact, in such flows the dissipation is nearly isotropic and it is logical that the rotation does not affect ϵ because of the analogy of each direction. At low Reynolds number, the dissipation becomes non-isotropic, both the effects of Reynolds number and Richardson number may be important in this case.



Secondly, it appears that the effects of rotation are more important on the production terms than on the others. In fact, if we examine equation 17 it is easy to show that the Reynolds stresses may be greatly affected by the rotation while the kinetic energy and its dissipation rate are not so much affected. Then it is evident that the most important relation which controls the calculation is the eddy viscosity coefficient.

Thirdly, we may make another remark which is also related to the preceding comment. The analysis of the dissipation equation shows that the effect of rotation should affect the "production" term instead of the "dissipation" term in the equation for ϵ . Most of the models at the present time account for the rotation through the "dissipation" term [see Launder, Priddin, Sharma (1977); Howard, Patankar, Bordyniuk (1980)]. Nevertheless, our analysis seems to be in accord with the remark which was made by Launder et al. (1977) that the corrections might have been better made on the "production" term of the ϵ equation instead of on the decay part.

A computer code has been written to check the model presented here, in simple cases such as flat plate boundary layers, boundary layers on rotating cylinder. The program is based on the Patankar-Spalding procedure (1970) and is used to solve the parabolic transport equations for the velocities, the kinetic energy and its dissipation. It is operational for two dimensional boundary layers on flat plates, and is being modified to calculate boundary layers on rotating cylinder. These calculations are performed in order to check the assumptions made for low Reynolds number modeling. Then the model could be included in the three-dimensional computer codes developed at Penn State.

3. MEASUREMENTS OF THE THREE DIMENSIONAL FLOW INSIDE AN AXIAL FLOW COMPRESSOR ROTOR PASSAGE

Experimental Program

The measurements reported in this report were performed using the Axial Flow Compressor facility in the Department of Aerospace Engineering.

The flow is surveyed across the entire passage at six axial locations (one upstream, four inside the rotor passage, and one downstream) and at five radial locations. Measurements were taken at five radial locations ($R = 0.58, 0.67, 0.75, 0.83, 0.918$) at each of the following axial stations inside the passage: $Z = -0.5$ (upstream), 0.26, 0.5, 0.73, 0.97, and 1.06.

The data inside and downstream of the rotor were acquired with a five-hole probe, rotating with the rotor. The data upstream were acquired with a stationary five-hole probe. All the measurements were taken at the design flow coefficient $\phi = 0.56$.

The results of the measurements are compared with the predictions from the Katsanis and McNally (1977) computer program.

Typical Results

A small sample of the experimental data and some comparisons with the predictions from the Katsanis and McNally (1977) program are presented here.

The measured and predicted blade to blade distributions of the axial (WZ), tangential (WT) and radial (WR) relative velocity at $R = 0.918$ (near the tip) and at $Z = 0.26, 0.5, 0.73, 0.97$ are shown in Figures 1 through 4. All the components of velocity are normalized with respect to the tip speed velocity. The predictions for the axial velocity are quite good at the

last two axial stations (i.e., $Z = 0.73, 0.93$). At the first two axial stations, the agreement is only reasonable and the slope of the predicted and measured profiles are of opposite sign.

The predictions for the tangential velocity are quite good except at the last axial station $Z = 0.97$. Nevertheless, at this location the shape of the predicted and measured profiles are strikingly identical. The difference in magnitude comes from the fact that the code cannot predict the flow near the trailing edge accurately. This is because it cannot incorporate the Kutta condition correctly, since it is based on an inviscid analysis.

The program does not have the ability to predict blade to blade distributions of radial velocity. The predicted radial velocity profiles that are shown in Figures 1 through 4 are computed by assuming that the meridional angle calculated in the S_2 surface solution is constant along the entire blade passage.

The measured blade to blade distributions of the relative total pressure and the static pressure are shown in Figures 5 through 8. Both the total and the static pressure are normalized by $1/2 \rho U_t^2$.

The static pressure profiles are fairly linear with the loading decreasing as we go from $Z = 0.26$ to $Z = 0.97$.

The relative total pressure profiles are almost flat. The mean value of relative total pressure is almost constant. The difference of the mean relative total pressure at $Z = 0.26$ and $Z = 0.97$ is less than 1 percent. This indicates that the losses in the inviscid part of the flow through the blade passage are very small.

The measured profiles of the axial, tangential, and radial relative velocity downstream of the rotor are shown in Figures 9 through 13. The axial location is not the same for different radial locations due to the geometrical constraint on the probe.

The velocity defect is maximum at the location $Z = 1.049$, $R = 0.587$ and minimum at the location $Z = 1.085$, $R = 0.918$.

The radial velocity is less than 10 percent of the tip speed velocity at all locations and mostly outwards. This agrees well with measurements taken by Dring et al. (1981) and Davino and Lakshminarayana (1981). Small inward radial velocity at the pressure side region can be seen at the radial locations nearest to the hub and casing while in the mid-span region the radial velocity is everywhere outwards.

Inward radial velocity at the pressure side region is induced by the shed vorticity. Shed vorticity results from the gradient in blade loading across the span. Since the loading in the mid-span is relatively uniform, there is no strong shed vorticity in that region so inward radial velocity cannot exist. This justifies the present experimental results.

The measured profiles of the relative total pressure and the static pressure downstream of the rotor are shown in Figures 14 through 18. As it was expected the relative total pressure profiles follow the behavior of the axial and tangential velocity profiles.

The static pressure profiles show an increase of the static pressure in the wake region. This comes in contrast to the classical assumption of constant static pressure across the wake. Similar observation has been reported by Lakshminarayana and Davino (1980).

4. PAPERS, THESES, REPORTS PUBLISHED DURING
JULY 1981 - DECEMBER 1981

- B. Lakshminarayana and T. R. Govindan, "Analysis of Turbulent Boundary Layer on Cascade and Rotor Blades of Turbomachinery," AIAA Journal, Vol. 19, No. 10, pp. 1333-1341, October 1981.
- C. Hah, "Three Dimensional Structures and Turbulence Closure of the Wake Developing in a Wall Shear Layer," AIAA Paper 81-1269, 1981.

REFERENCES

- Alcaraz, E. (1977), "Contribution a l'etude d'un jet plan turbulent evoluant le long d'une paroi convexe a faible courbure," These d'Etat, Univ. Claude Bernard, Lyon.
- Anand, A. K. and Lakshminarayana, B. (1975), "Three-dimensional boundary layer in a rotating helical channel," Journal of Fluids Engineering, Vol. 97, No. 2.
- Anand, A. K. and Lakshminarayana, B. (1978), "An experimental study of three-dimensional turbulent boundary layer and turbulence characteristics inside a turbomachinery rotor passage," Journal of Engineering for Power, Vol. 100.
- Arzoumanian, E., Fulachier, L., and Dumas, R. (1979), "Experimental investigation of the three dimensional turbulent boundary layer on an axially rotated cylinder," Second International Symposium on Turbulent Shear Flows, The Pennsylvania State University.
- Bertoglio, J. P. (1980), "Homogeneous turbulent field within a rotating frame," AIAA 13th Fluid and Plasma Dynamics Conference.
- Bertoglio, J. P., Charnay, G., and Mathieu, J. (1980), "Effets de la rotation sur un champ turbulent cisaille: application au casdes turbomachines," Journal de Mecanique Appliquee, Vol. 4, No. 4.
- Bissonnette, L. R. and Mellor, G. L. (1970), "Experiments on the behavior of an axisymmetric turbulent boundary layer with a sudden circumferential strain," Journal of Fluid Mechanics, Vol. 63, Pt. 2, pp. 269-413.
- Bradshaw, P. (1969), "The analogy between stream curvature and buoyancy in turbulent shear flows," Journal of Fluid Mechanics, Vol. 36, Pt. 1, p. 177.
- Bradshaw, P. (1977), "Compressible turbulent shear layers," Annual Review of Fluid Mechanics.
- Briley, W. R. and McDonald, H. (1979), "On the structure and use of linearized block implicit schemes," Journal Comp. Phys., Vol. 34, pp. 54-73.
- Castro, I. P. and Bradshaw, P. (1976), "The turbulence structure of a highly curved mixing layer," Journal of Fluid Mechanics, Vol. 73, pp. 265-304.
- Chou, P. Y. (1945), "On velocity correlations and the solutions of the equations of turbulent fluctuation," Quarterly of Applied Mathematics, Vol. 3, No. 38.
- Cousteix, J. and Aupoix, B. (1979), "Comparison of various calculation methods for three dimensional turbulent boundary layer," Second Symposium on Turbulent Shear Flows, The Pennsylvania State University.

- Daly, B. J. and Harlow, F. H. (1970), "Transport equations in turbulence," The Physics of Fluids, Vol. 13, No. 11.
- Davino, R. and Lakshminarayana, B. (1981), "Characteristics of mean velocity in the annulus wall region at the exit of turbomachinery rotor passage," AIAA Paper 81-0068 (to be published in AIAA Journal, 1982).
- Dring, R. P., Joslyn, H. D., and Hardin, L. W. (1981), "An investigation of axial compressor rotor aerodynamics," ASME Paper 81-GT-56.
- Gibson, M. M. (1978), "An algebraic stress and heat-flux model for turbulent shear flow with streamline curvature," Int. Journal of Heat and Mass Transfer, Vol. 21.
- Gibson, M. M. and Rodi, W. (1981), "A Reynolds-stress closure model of turbulence applied to the calculation of a highly curved mixing layer," Journal of Fluid Mechanics, Vol. 103.
- Gibson, M. M. and Younis, B. A. (1981), "Calculation of a turbulent wall jet on a curved wall with a Reynolds stress model of turbulence," Mechanical Engineering Department, Imperial College.
- Gibson, M. M., Jones, W. P., and Younis, B. A. (1981), Physics of Fluids, Vol. 24, No. 3, p. 386.
- Görtler, (1959), Ing. Arch., No. 28.
- Hah, C. and Lakshminarayana, B. (1980), "Numerical analysis of turbulent wakes of turbomachinery rotor blades," Journal of Fluids Engineering, Vol. 102.
- Hah, C. (1981), "Three-dimensional structures and turbulence closure of the wake developing in a wall shear layer," AIAA 14th Fluid and Plasma Conference, AIAA Paper 81-1269.
- Hanjalic, K. and Launder, B. E. (1972), "A Reynolds stress model of turbulence and its application to thin shear flows," Journal of Fluid Mechanics, Vol. 52, Pt. 4.
- Hanjalic, K. and Launder, B. E. (1978), "Turbulent transport modeling of separating and reattaching shear flows," Report TF/78/8, University of California at Davis.
- Hoffman, P. M. and Bradshaw, P. (1978), "Turbulent boundary layers on surfaces of mild longitudinal curvature," Aerospace Report 78-04, Imperial College.
- Howard, J. H. G., Patankar, S. V., and Bordinuik, R. M. (1980), "Flow prediction in rotating ducts using Coriolis-modified turbulence models," ASME Journal of Fluids Engineering.
- Hunt, I. A. and Joubert, P. N. (1979), "Effects of small streamline curvature on turbulent duct flow," Journal of Fluid Mechanics, Vol. 91, Pt. 4.

- I-Man Moon, (1964), "Effect of Coriolis force on the turbulent boundary layer in rotating fluid machines," Report No. 74, Massachusetts Institute of Technology.
- Irwin, H. P. A. H. and Smith, P. A. (1975), "Prediction of the effect of streamline curvature on turbulence," Physics of Fluids, Vol. 18.
- Johnston, J. P. (1970), Thermosciences Division, Mechanical Engineering Department, Stanford University, Report MD24.
- Johnston, J. P., Halleen, R. M., and Lezius, D. K. (1972), "Effect of spanwise rotation on the structure of two dimensional fully developed turbulent channel flow," Journal of Fluid Mechanics, Vol. 56, Pt. 3.
- Jones, W. P. and Launder, B. E. (1972), "The prediction of laminarization with a two-equation model of turbulence," International Journal of Heat and Mass Transfer, Vol. 15.
- Katsanis, T. and McNally, W. (1977), "Revised Fortran program for calculating velocities and streamlines on the hub-shroud mid-channel stream surface of an axial-, radial-, and mixed-flow turbomachine or annular duct," NASA TND 8430.
- Koosilin, M. L. and Lockwood, F. C. (1974), "The prediction of axisymmetric turbulent swirling boundary layers," AIAA Journal, Vol. 12, No. 4.
- Koyama, M., Masuda, S., Ariga, I., and Watanabe, I. (1979), "Turbulence structure and three dimensionality of a rotating two-dimensional turbulent boundary layer," Second Symposium on Turbulent Shear Flow, London.
- Lakshminarayana, B. and Davino, R. (1980), "Mean velocity and decay characteristics of the guidevane and stator blade wake of an axial flow compressor," Journal of Engineering for Power, Vol. 102, pp. 50-60.
- Lakshminarayana, B., Jabbari, A., and Yamaoka, H. (1972), "Turbulent boundary layer on a rotating helical blade," Journal of Fluid Mechanics, Vol. 51, Pt. 3.
- Lakshminarayana, B. and Reynolds, B. (1979), "Turbulent characteristics in the near wake of a compressor rotor blade," AIAA Journal, Vol. 18, No. 11.
- Lakshminarayana, B. and Govindan, T. R. (1981), "Analysis of turbulent boundary layer on cascade and rotor blades of turbomachinery," Fifth International Symposium on Airbreathing Engines, Bangalore.
- Launder, B. E., Reece, G. J., and Rodi, W. (1975), "Progress in the development of a Reynolds stress turbulence closure," Journal of Fluid Mechanics, Vol. 68, Pt. 3.

- Launder, B. E., Priddin, C. H., and Sharma, B. I. (1977), "The calculation of turbulent boundary layers on spinning and curved surfaces," ASME Journal of Fluids Engineering.
- Launder, B. E. and Morse, A. (1979), "Numerical prediction of axisymmetric free shear flows with a second order Reynolds-stress closure," Proc. First Symposium on Turbulent Shear Flows, Heidelberg.
- Lohmann, R. P. (1973), "The response of developed turbulent boundary layer to local transverse surface motion," Ph.D. Thesis, University of Connecticut.
- Lumley, J. L. (1970), "Toward a turbulent constitutive relation," Journal of Fluid Mechanics, Vol. 41, Pt. 2.
- Lumley, J. L. and Khajeh-Nouri, B. (1974), "Computational modeling of turbulent transport," Advances in Geophysics, Vol. 18A.
- Majumdar, A. K., Pratap, V. S., and Spalding, D. B. (1977), "Numerical computation of flow in rotating ducts," ASME Journal of Fluids Engineering.
- Majumdar, A. K. and Spalding, D. B. (1977), "A numerical investigation of three-dimensional flows in a rotating duct by a partially-parabolic procedure," ASME Paper 77-WA/FE-7.
- Margolis, D. P. (1963), "An investigation of a curved mixing layer," Ph.D. Thesis, The Pennsylvania State University.
- Moore, J. (1973), "A wake and an eddy in a rotating radial flow passage-Part 1: Experimental observations," ASME Paper No. 73-GT-57.
- Murakami, M., Kikyama, K., and Nishibori, K. (1981), "Three-dimensional boundary layer development in an axially rotating pipe," Department of Mechanical Engineering, Nagoya University, Japan.
- Nakamura, I., Yamashita, S., Watanabe, T., and Sawaki, Y. (1981), "Three-dimensional turbulent boundary layer on a spinning thin cylinder in an axial uniform stream," Department of Mechanical Engineering, Nagoya University and Mie University, Japan.
- Nakano, S., Takahashi, A., Shizawa, T., and Honami, S. (1981), "Effects of stable and unstable free streams on a turbulent flow over a concave surface," Department of Mechanical Engineering, University of Tokyo.
- Patankar, S. V. and Spalding, D. B. (1970), Heat and Mass Transfer in Boundary Layers, A General Calculation Procedure, Intertext Book, London.

- Patankar, S. V. and Spalding, D. B. (1972), "A calculation method for heat, mass and momentum transfer in three-dimensional parabolic flows," International Journal of Heat and Mass Transfer, Vol. 15.
- Prandtl, L. (1930), Reprint in L. Prandtl gesammelte Abhandlungen 2, 778, Berlin, Springer, 1961.
- Raj, R. (1975), "Form of the turbulence dissipation equation as applied to curved and rotating turbulent flows," Department of Mechanical Engineering, City University of New York, New York.
- Raj, R. and Lakshminarayana, B. (1975), "On the investigation of cascade and turbomachinery rotor wake characteristics," NASA CR 134680.
- Ravindranath, A. and Lakshminarayana, B. (1980), "Mean velocity and decay characteristics of the near wake and far wake of a compressor rotor blade of moderate loading," Journal of Engineering for Power, Vol. 102.
- Sharma, B. I. (1977), "Computation of flow past a rotating cylinder with an energy-dissipation model of turbulence," AIAA Journal, Vol. 15, No. 2.
- So, R. M. C. and Mellor, G. L. (1975), "Experiment on turbulent boundary layers on a concave wall," Aeronautical Quarterly, Vol. 26.
- Spitz, P. (1980), "Etude numerique et experimentale d'un ecoulement turbulent complexe: couche limite soumise a un brusque cisaillement transversal," These 3eme cycle IMST, Marseille, France.
- Townsend, A. A. (1980), "The response of sheared turbulence to additional distortion," Journal of Fluid Mechanics, Vol. 98.
- Tennekes, H. and Lumley, J. L. (1972), A First Course in Turbulence, M.I.T. Press, Cambridge.
- Wilcox, D. C. and Chambers, T. L. (1977), "Streamline curvature effects on turbulent boundary layers," AIAA Journal, Vol. 15, No. 4.

APPENDIX 1

Transformed Momentum Equations and Jacobian Matrices

Momentum Equation in z-Direction

$$\frac{\partial}{\partial z}(\rho U^2) + \frac{\partial}{r \partial \theta}(\rho UV) + \frac{\partial}{\partial r}(\rho UW) + \frac{\rho UW}{r} = - \frac{\partial P}{\partial z} + \frac{1}{Re} \left[\frac{\partial}{\partial r} \left[\mu \left(\frac{\partial U}{\partial r} + \frac{\partial W}{\partial z} \right) \right] + \frac{\partial}{r \partial \theta} \left[\mu \left(\frac{\partial V}{\partial z} + \frac{\partial U}{r \partial \theta} \right) \right] \right. \\ \left. + \frac{\partial}{\partial z} \left[2\mu \frac{\partial U}{\partial z} - \frac{2}{3} \mu \left[\frac{\partial V}{\partial r} + \frac{\partial V}{r \partial \theta} + \frac{\partial U}{\partial z} + \frac{W}{r} \right] \right] + \frac{\mu}{r} \left(\frac{\partial U}{\partial r} + \frac{\partial W}{\partial z} \right) \right]$$

The coordinate transformation is of the form

$$\xi = \xi(z, r\theta) \equiv \xi(z, \theta)$$

$$\eta = \eta(z, r\theta) \equiv \eta(z, \theta)$$

$$R = R(r) \equiv R(r)$$

ξ , η , R are the transformed coordinates in the streamwise, normal, and radial directions, respectively.

$$\frac{\partial}{\partial z} = \frac{\partial}{\partial \xi} \xi_z + \frac{\partial}{\partial \eta} \eta_z$$

$$\frac{\partial}{\partial \theta} = \frac{\partial}{\partial \xi} \xi_\theta + \frac{\partial}{\partial \eta} \eta_\theta$$

$$\frac{\partial}{\partial r} = \frac{\partial}{\partial R} R_r$$

$$\text{L.H.S.} = \xi_z \frac{\partial}{\partial \xi}(\rho U^2) + \eta_z \frac{\partial}{\partial \eta}(\rho U^2) + \xi_\theta \frac{\partial}{\partial \xi}(\rho UV) + \eta_\theta \frac{\partial}{\partial \eta}(\rho UV) + R_r \frac{\partial}{\partial R}(\rho UW) + \frac{\rho UW}{R} \\ = \frac{\partial}{\partial \xi} \left(\frac{\xi_z}{J} \rho U^2 + \frac{\xi_\theta}{J} \rho UV \right) + \frac{\partial}{\partial \eta} \left(\frac{\eta_z}{J} \rho U^2 + \frac{\eta_\theta}{J} \rho UV \right) + \frac{\partial}{\partial R} \left(\frac{R_r}{J} \rho UW \right) + \frac{\rho UW}{R}$$

$$\begin{aligned}
\text{R.H.S.} = & - \left(\xi_z \frac{\partial P}{\partial \xi} + \eta_z \frac{\partial P}{\partial \eta} \right) + \frac{1}{\text{Re}} \left[\frac{\partial}{\partial R} \left[\frac{R_r}{J} \left[\mu \left(R_r \frac{\partial U}{\partial R} + \xi_z \frac{\partial W}{\partial \xi} + \eta_z \frac{\partial W}{\partial \eta} \right) \right] \right] \right] \\
& + \xi_\theta \frac{\partial}{\partial \xi} \left[\mu \left(\xi_z \frac{\partial V}{\partial \xi} + \eta_z \frac{\partial V}{\partial \eta} + \xi_\theta \frac{\partial U}{\partial \xi} + \eta_\theta \frac{\partial U}{\partial \eta} \right) \right] \\
& + \eta_\theta \frac{\partial}{\partial \eta} \left[\mu \left(\xi_z \frac{\partial V}{\partial \xi} + \eta_z \frac{\partial V}{\partial \eta} + \xi_\theta \frac{\partial U}{\partial \xi} + \eta_\theta \frac{\partial U}{\partial \eta} \right) \right] \\
& + \xi_z \frac{\partial}{\partial \xi} \left[2\mu \left(\xi_z \frac{\partial U}{\partial \xi} + \eta_z \frac{\partial U}{\partial \eta} \right) - \frac{2}{3} \mu \left(R_r \frac{\partial W}{\partial R} \right. \right. \\
& \left. \left. + \xi_\theta \frac{\partial V}{\partial \xi} + \eta_\theta \frac{\partial V}{\partial \eta} + \xi_z \frac{\partial U}{\partial \xi} + \eta_z \frac{\partial U}{\partial \eta} + \frac{W}{R} \right) \right] \\
& + \eta_z \frac{\partial}{\partial \eta} \left[2\mu \left(\xi_z \frac{\partial U}{\partial \xi} + \eta_z \frac{\partial U}{\partial \eta} \right) - \frac{2}{3} \mu \left(R_r \frac{\partial W}{\partial R} \right. \right. \\
& \left. \left. + \xi_\theta \frac{\partial V}{\partial \xi} + \eta_\theta \frac{\partial V}{\partial \eta} + \xi_z \frac{\partial U}{\partial \xi} + \eta_z \frac{\partial U}{\partial \eta} + \frac{W}{R} \right) \right] \\
& + \frac{\mu}{R} \left[R_r \frac{\partial U}{\partial R} + \xi_z \frac{\partial W}{\partial \xi} + \eta_z \frac{\partial W}{\partial \eta} \right]
\end{aligned}$$

Dropping the diffusion terms in the ξ direction, we get,

$$\begin{aligned}
\text{R.H.S.} = & - \left(\xi_z \frac{\partial P}{\partial \xi} + \eta_z \frac{\partial P}{\partial \eta} \right) + \frac{1}{\text{Re}} \left[\frac{\partial}{\partial R} \left[\frac{R_r}{J} \left[\mu \left(R_r \frac{\partial U}{\partial R} + \eta_z \frac{\partial W}{\partial \eta} \right) \right] \right] \right] \\
& + \eta_\theta \frac{\partial}{\partial \eta} \left[\mu \left(\eta_z \frac{\partial V}{\partial \eta} + \eta_\theta \frac{\partial U}{\partial \eta} \right) \right] \\
& + \eta_z \frac{\partial}{\partial \eta} \left[2\mu \eta_z \frac{\partial U}{\partial \eta} - \frac{2}{3} \mu \left(R_r \frac{\partial W}{\partial R} + \eta_\theta \frac{\partial V}{\partial \eta} + \eta_z \frac{\partial U}{\partial \eta} + \frac{W}{R} \right) \right] \\
& + \frac{\mu}{R} \left[R_r \frac{\partial U}{\partial R} + \eta_z \frac{\partial W}{\partial \eta} \right]
\end{aligned}$$

$$\begin{aligned}
& - \left(\xi_z \frac{\partial P}{\partial \xi} + \eta_z \frac{\partial P}{\partial \eta} \right) + \frac{1}{Re} \left[R_r \frac{\partial}{\partial R} \left[\mu \left(R_r \frac{\partial U}{\partial R} + \eta_z \frac{\partial W}{\partial \eta} \right) \right] \right] \\
& + \frac{\partial}{\partial \eta} \left[\mu \left(\frac{\eta_z \eta_\theta}{J} \frac{\partial V}{\partial \eta} + \frac{\eta_\theta^2}{J} \frac{\partial U}{\partial \eta} \right) + 2\mu \frac{\eta_z^2}{J} \frac{\partial U}{\partial \eta} \right. \\
& \left. - \frac{2}{3} \mu \frac{\eta_z}{J} \left(R_r \frac{\partial W}{\partial r} + \eta_\theta \frac{\partial V}{\partial \eta} + \eta_z \frac{\partial U}{\partial \eta} + \frac{W}{R} \right) \right] + \frac{\mu}{R} \left[R_r \frac{\partial U}{\partial R} + \eta_z \frac{\partial W}{\partial \eta} \right] \\
& - \left(\xi_z \frac{\partial P}{\partial \xi} + \eta_z \frac{\partial P}{\partial \eta} \right) + \frac{1}{Re} \left[\frac{\partial}{\partial R} \left[\frac{R_r}{J} \left[\mu \left(R_r \frac{\partial U}{\partial R} + \eta_z \frac{\partial W}{\partial \eta} \right) \right] \right] \right] \\
& + \frac{\partial}{\partial \eta} \left[\mu \left[\frac{\eta_z \eta_\theta}{J} \frac{\partial V}{\partial \eta} + \frac{\eta_\theta^2}{J} \frac{\partial U}{\partial \eta} + 2 \frac{\eta_z^2}{J} \frac{\partial U}{\partial \eta} - \frac{2}{3} \frac{\eta_z}{J} R_r \frac{\partial W}{\partial r} - \frac{2}{3} \frac{\eta_z \eta_\theta}{J} \frac{\partial V}{\partial \eta} \right. \right. \\
& \left. \left. - \frac{2}{3} \frac{\eta_z^2}{J} \frac{\partial U}{\partial \eta} - \frac{2}{3} \frac{\eta_z}{J} \frac{W}{R} \right] + \frac{\mu}{R} \left[R_r \frac{\partial U}{\partial R} + \eta_z \frac{\partial W}{\partial \eta} \right] \right] \\
& - \left[\xi_z \frac{\partial P}{\partial \xi} + \eta_z \frac{\partial P}{\partial \eta} \right] + \frac{1}{Re} \left[R_r \frac{\partial}{\partial R} \left[\mu \left(R_r \frac{\partial U}{\partial R} + \eta_z \frac{\partial W}{\partial \eta} \right) \right] \right] \\
& + \frac{\partial}{\partial \eta} \left[\mu \left(\frac{[\eta_\theta^2 + \eta_z^2]}{J} \frac{\partial U}{\partial \eta} + \frac{1}{3} \frac{\eta_z}{J} \left(\eta_\theta \frac{\partial V}{\partial \eta} + \eta_z \frac{\partial U}{\partial \eta} \right) - \frac{2}{3} \frac{\eta_z}{J} \left(R_r \frac{\partial W}{\partial r} + \frac{W}{R} \right) \right) \right. \\
& \left. + \frac{\mu}{R} \left[R_r \frac{\partial U}{\partial R} + \eta_z \frac{\partial W}{\partial \eta} \right] \right]
\end{aligned}$$

The complete transformed z-momentum equation is

$$\begin{aligned}
& \frac{\partial}{\partial \xi} \left(\xi_z \rho U^2 + \frac{\xi_\theta}{J} \rho UV \right) + \frac{\partial}{\partial \eta} \left(\eta_z \rho U^2 + \frac{\eta_\theta}{J} \rho UV \right) + \frac{\partial}{\partial R} \left(\frac{R_r}{J} \rho UW \right) + \frac{\rho UW}{R} + \frac{\partial}{\partial \xi} \left(\xi_z \rho \right) \\
& + \frac{\partial}{\partial \eta} \left(\eta_z \rho \right) - \frac{1}{Re} \left[\frac{\partial}{\partial R} \left[\frac{R_r}{J} \left[\mu \left(R_r \frac{\partial U}{\partial R} + \eta_z \frac{\partial W}{\partial \eta} \right) \right] \right] \right] \\
& + \frac{\partial}{\partial \eta} \left[\mu \left(\frac{[\eta_\theta^2 + \eta_z^2]}{J} \frac{\partial U}{\partial \eta} + \frac{1}{3} \frac{\eta_z}{J} \left(\eta_\theta \frac{\partial V}{\partial \eta} + \eta_z \frac{\partial U}{\partial \eta} \right) - \frac{2}{3} \frac{\eta_z}{J} \left(R_r \frac{\partial W}{\partial r} + \frac{W}{R} \right) \right) \right. \\
& \left. + \frac{\mu}{R} \left[R_r \frac{\partial U}{\partial R} + \eta_z \frac{\partial W}{\partial \eta} \right] \right]
\end{aligned}$$

Momentum Equation in θ Direction

$$\begin{aligned} \frac{\partial}{\partial z}(\rho UV) + \frac{\partial}{r\partial\theta}(\rho V^2) + \frac{\partial}{\partial r}(\rho VW) + \frac{2\rho VW}{r} + 2\rho\Omega W - \frac{\partial P}{r\partial\theta} + \frac{1}{Re} \left[\frac{\partial}{\partial r} \left(\mu \left(\frac{\partial W}{r\partial\theta} + r \frac{\partial}{\partial r} \left(\frac{V}{r} \right) \right) \right) \right. \\ \left. + \frac{\partial}{r\partial\theta} \left(2\mu \left(\frac{\partial V}{r\partial\theta} + \frac{W}{r} \right) - \frac{2}{3} \mu \left[\frac{\partial W}{\partial r} + \frac{\partial V}{r\partial\theta} + \frac{\partial U}{\partial z} + \frac{W}{r} \right] + \frac{\partial}{\partial z} \left(\mu \left[\frac{\partial V}{\partial z} + \frac{\partial U}{r\partial\theta} \right] \right) \right. \right. \\ \left. \left. + \frac{2\mu}{r} \left(\frac{\partial W}{r\partial\theta} + r \frac{\partial}{\partial r} \left(\frac{V}{r} \right) \right) \right] \right] \end{aligned}$$

Transferring from r, θ, z coordinate system to R, η, ξ coordinate system with $R = R(r), \eta = \eta(z, r\theta) \equiv \eta(z, \theta), \xi = \xi(z, r\theta) \equiv \xi(z, \theta)$ we get

$$\begin{aligned} \text{L.H.S.} &= \xi_z \frac{\partial}{\partial \xi}(\rho UV) + \eta_z \frac{\partial}{\partial \eta}(\rho UV) + \xi_\theta \frac{\partial}{\partial \xi}(\rho V^2) + \eta_\theta \frac{\partial}{\partial \eta}(\rho V^2) \\ &\quad + \frac{\partial}{\partial R} \left(\frac{Rr}{J} \rho VW \right) + \frac{2\rho VW}{R} + 2\rho\Omega W \\ &= \frac{\partial}{\partial \xi} \left(\frac{\xi_z}{J} \rho UV + \frac{\xi_\theta}{J} \rho V^2 \right) + \frac{\partial}{\partial \eta} \left(\frac{\eta_z}{J} \rho UV + \frac{\eta_\theta}{J} \rho V^2 \right) + \frac{\partial}{\partial R} \left(\frac{Rr}{J} \rho VW \right) + \frac{2\rho VW}{R} + 2\rho\Omega W \end{aligned}$$

$$\begin{aligned} \text{R.H.S.} &= - \left(\xi_\theta \frac{\partial P}{\partial \xi} + \eta_\theta \frac{\partial P}{\partial \eta} \right) + \frac{1}{Re} \left[\frac{\partial}{\partial R} \frac{Rr}{J} \left[\mu \left[\xi_\theta \frac{\partial W}{\partial \xi} + \eta_\theta \frac{\partial W}{\partial \eta} + Rr \frac{\partial V}{\partial R} - \frac{V}{R} \right] \right] \right. \\ &\quad + \xi_\theta \frac{\partial}{\partial \xi} \left[2\mu \left(\xi_\theta \frac{\partial V}{\partial \xi} + \eta_\theta \frac{\partial V}{\partial \eta} + \frac{W}{R} \right) - \frac{2}{3} \mu \left[Rr \frac{\partial W}{\partial R} \right. \right. \\ &\quad \left. \left. + \xi_\theta \frac{\partial V}{\partial \xi} + \eta_\theta \frac{\partial V}{\partial \eta} + \xi_z \frac{\partial U}{\partial \xi} + \eta_z \frac{\partial U}{\partial \eta} + \frac{W}{R} \right] \right. \\ &\quad + \eta_\theta \frac{\partial}{\partial \eta} \left[2\mu \left(\xi_\theta \frac{\partial V}{\partial \xi} + \eta_\theta \frac{\partial V}{\partial \eta} + \frac{W}{R} \right) - \frac{2}{3} \mu \left[Rr \frac{\partial W}{\partial R} \right. \right. \\ &\quad \left. \left. + \xi_\theta \frac{\partial V}{\partial \xi} + \eta_\theta \frac{\partial V}{\partial \eta} + \xi_z \frac{\partial U}{\partial \xi} + \eta_z \frac{\partial U}{\partial \eta} + \frac{W}{R} \right] \right. \\ &\quad + \xi_z \frac{\partial}{\partial \xi} \left(\mu \left[\xi_z \frac{\partial V}{\partial \xi} + \eta_z \frac{\partial V}{\partial \eta} + \xi_\theta \frac{\partial U}{\partial \xi} + \eta_\theta \frac{\partial U}{\partial \eta} \right] \right) \\ &\quad + \eta_z \frac{\partial}{\partial \eta} \left(\mu \left[\xi_z \frac{\partial V}{\partial \xi} + \eta_z \frac{\partial V}{\partial \eta} + \xi_\theta \frac{\partial U}{\partial \xi} + \eta_\theta \frac{\partial U}{\partial \eta} \right] \right) \\ &\quad \left. + \frac{2\mu}{R} \left(\xi_\theta \frac{\partial W}{\partial \xi} + \eta_\theta \frac{\partial W}{\partial \eta} + Rr \frac{\partial V}{\partial R} - \frac{V}{R} \right) \right] \end{aligned}$$

Dropping the diffusion terms in the ξ direction, we get,

$$\begin{aligned}
\text{R.H.S.} &= -\left(\xi_\theta \frac{\partial P}{\partial \xi} + \eta_\theta \frac{\partial P}{\partial \eta}\right) + \frac{1}{\text{Re}} \left[\frac{\partial}{\partial R} \left(\frac{R_r}{J} \left[\mu \left(\eta_\theta \frac{\partial W}{\partial \eta} + R_r \frac{\partial V}{\partial R} - \frac{V}{R} \right) \right] \right) \right] \\
&+ \eta_\theta \frac{\partial}{\partial \eta} \left[2\mu \left(\eta_\theta \frac{\partial V}{\partial \eta} + \frac{W}{R} \right) - \frac{2}{3} \mu \left[R_r \frac{\partial W}{\partial R} + \eta_\theta \frac{\partial V}{\partial \eta} + \eta_z \frac{\partial U}{\partial \eta} + \frac{W}{R} \right] \right] \\
&+ \eta_z \frac{\partial}{\partial \eta} \left[\mu \left(\eta_z \frac{\partial V}{\partial \eta} + \eta_\theta \frac{\partial U}{\partial \eta} \right) \right] + \frac{2\mu}{R} \left(\eta_\theta \frac{\partial W}{\partial \eta} + R_r \frac{\partial V}{\partial R} - \frac{V}{R} \right) \\
&= -\left(\xi_\theta \frac{\partial P}{\partial \xi} + \eta_\theta \frac{\partial P}{\partial \eta}\right) + \frac{1}{\text{Re}} \left[\frac{\partial}{\partial R} \left(\frac{R_r}{J} \right) \left[\mu \left(\eta_\theta \frac{\partial W}{\partial \eta} + R_r \frac{\partial V}{\partial R} - \frac{V}{R} \right) \right] \right] \\
&+ \frac{\partial}{\partial \eta} \left[2\mu \frac{\eta_\theta}{J} \left(\eta_\theta \frac{\partial V}{\partial \eta} + \frac{W}{R} \right) - \frac{2\mu\eta_\theta}{3J} \left[R_r \frac{\partial W}{\partial R} + \eta_\theta \frac{\partial V}{\partial \eta} + \eta_z \frac{\partial U}{\partial \eta} + \frac{W}{R} \right] \right] \\
&+ \mu \frac{\eta_z}{J} \left(\eta_z \frac{\partial V}{\partial \eta} + \eta_\theta \frac{\partial U}{\partial \eta} \right) + \frac{2\mu}{R} \left[\eta_\theta \frac{\partial W}{\partial \eta} + R_r \frac{\partial V}{\partial R} - \frac{V}{R} \right] \\
&= -\left(\xi_\theta \frac{\partial P}{\partial \xi} + \eta_\theta \frac{\partial P}{\partial \eta}\right) + \frac{1}{\text{Re}} \left[\frac{\partial}{\partial R} \left(\frac{R_r}{J} \left[\mu \left(\eta_\theta \frac{\partial W}{\partial \eta} + R_r \frac{\partial V}{\partial R} - \frac{V}{R} \right) \right] \right) \right] + \frac{\partial}{\partial \eta} \left[\frac{2\mu\eta_\theta^2}{J} \frac{\partial V}{\partial \eta} \right] \\
&+ 2\mu \frac{\eta_\theta}{J} \frac{W}{R} - \frac{2\mu\eta_\theta}{3J} \left(R_r \frac{\partial W}{\partial R} + \frac{W}{R} \right) - \frac{2\mu\eta_\theta^2}{3J} \frac{\partial V}{\partial \eta} - \frac{2\mu\eta_\theta\eta_z}{3J} \frac{\partial U}{\partial \eta} + \mu \frac{\eta_z^2}{J} \frac{\partial V}{\partial \eta} \\
&+ \mu \frac{\eta_z\eta_\theta}{J} \frac{\partial U}{\partial \eta} + \frac{2\mu}{R} \left[\eta_\theta \frac{\partial W}{\partial \eta} + R_r \frac{\partial V}{\partial R} - \frac{V}{R} \right]]]
\end{aligned}$$

The complete transformed θ -momentum equation is

$$\begin{aligned}
&\frac{\partial}{\partial \xi} \left(\frac{\xi_z}{J} \rho UV + \frac{\xi_\theta}{J} \rho V^2 \right) + \frac{\partial}{\partial \eta} \left(\frac{\eta_z}{J} \rho UV + \frac{\eta_\theta}{J} \rho V^2 \right) + \frac{\partial}{\partial R} \left(\frac{R_r}{J} \rho VW \right) + \rho VW \frac{2}{R} + 2\rho\Omega W \\
&+ \frac{\partial}{\partial \xi} \left(\frac{\xi_\theta}{J} P \right) + \frac{\partial}{\partial \eta} \left(\frac{\eta_\theta}{J} P \right) = \frac{1}{\text{Re}} \left[\frac{\partial}{\partial R} \left(\frac{R_r}{J} \left[\mu \left(\eta_\theta \frac{\partial W}{\partial \eta} + R_r \frac{\partial V}{\partial R} - \frac{V}{R} \right) \right] \right) \right] \\
&+ \frac{\partial}{\partial \eta} \left[\mu \left(\frac{\eta_\theta^2}{J} + \frac{\eta_z^2}{J} \right) \frac{\partial V}{\partial \eta} + \frac{\mu}{3} \frac{\eta_\theta}{J} \left(\eta_\theta \frac{\partial V}{\partial \eta} + \eta_z \frac{\partial U}{\partial \eta} \right) - \frac{2}{3} \mu \frac{\eta_\theta}{J} \left(R_r \frac{\partial W}{\partial R} + \frac{W}{R} \right) \right] \\
&+ 2\mu \frac{\eta_\theta}{J} \frac{W}{R} + \frac{2\mu}{R} \left[\eta_\theta \frac{\partial W}{\partial \eta} + R_r \frac{\partial V}{\partial R} - \frac{V}{R} \right]]
\end{aligned}$$

Momentum Equation in r-Direction

$$\begin{aligned} \frac{\partial}{\partial z}(\rho UW) + \frac{\partial}{r\partial\theta}(\rho VW) + \frac{\partial}{\partial r}(\rho W^2) + \frac{\rho(W^2 - V^2)}{r} - \rho\Omega^2 r - 2\rho\Omega V = -\frac{\partial P}{\partial r} + \frac{1}{Re} \left[\frac{\partial}{\partial r} \left[2\mu \frac{\partial W}{\partial r} \right. \right. \\ \left. \left. - \frac{2\mu}{3} \left[\frac{\partial W}{\partial r} + \frac{\partial V}{r\partial\theta} + \frac{\partial U}{\partial z} + \frac{W}{r} \right] \right] + \frac{\partial}{r\partial\theta} \left(\mu \left(\frac{\partial W}{r\partial\theta} + r \frac{\partial}{\partial r} \left(\frac{V}{r} \right) \right) \right) + \frac{\partial}{\partial z} \left(\mu \left(\frac{\partial U}{\partial r} + \frac{\partial W}{\partial z} \right) \right) \right. \\ \left. + \frac{1}{r} \left(2\mu \left[\frac{\partial W}{\partial r} - \frac{\partial V}{r\partial\theta} - \frac{W}{r} \right] \right) \right] \end{aligned}$$

going from r, θ, z to R, η, ξ we get

$$\begin{aligned} \text{L.H.S.} = \xi_z \frac{\partial}{\partial \xi}(\rho UW) + \eta_z \frac{\partial}{\partial \eta}(\rho UW) + \xi_\theta \frac{\partial}{\partial \xi}(\rho VW) + \eta_\theta \frac{\partial}{\partial \eta}(\rho VW) + \frac{\partial}{\partial R} \left(\frac{R}{J} \rho W^2 \right) \\ + \frac{\rho}{R} (W^2 - V^2) - \rho\Omega^2 R - 2\rho\Omega V \end{aligned}$$

$$\begin{aligned} = \frac{\partial}{\partial \xi} \left(\frac{\xi_z}{J} \rho UW + \frac{\xi_\theta}{J} \rho VW \right) + \frac{\partial}{\partial \eta} \left(\frac{\eta_z}{J} \rho UW + \frac{\eta_\theta}{J} \rho VW \right) + \frac{\partial}{\partial R} \left(\frac{R}{J} \rho W^2 \right) \\ + \frac{\rho}{R} (W^2 - V^2) - \rho\Omega^2 R - 2\rho\Omega V \end{aligned}$$

$$\begin{aligned} \text{R.H.S.} = -R_r \frac{\partial P}{\partial R} + \frac{1}{Re} \left[\frac{\partial}{\partial R} \frac{R}{J} \left[2\mu R_r \frac{\partial W}{\partial R} - \frac{2\mu}{3} \left[R_r \frac{\partial W}{\partial R} + \xi_\theta \frac{\partial V}{\partial \xi} + \eta_\theta \frac{\partial V}{\partial \eta} + \xi_z \frac{\partial U}{\partial \xi} + \eta_z \frac{\partial U}{\partial \eta} + \frac{W}{R} \right] \right. \right. \\ \left. \left. + \xi_\theta \frac{\partial}{\partial \xi} \left[\mu \left(\xi_\theta \frac{\partial W}{\partial \xi} + \eta_\theta \frac{\partial W}{\partial \eta} + R_r \frac{\partial V}{\partial R} - \frac{V}{R} \right) \right] \right. \right. \\ \left. \left. + \eta_\theta \frac{\partial}{\partial \eta} \left[\mu \left(\xi_\theta \frac{\partial W}{\partial \xi} + \eta_\theta \frac{\partial W}{\partial \eta} + R_r \frac{\partial V}{\partial R} - \frac{V}{R} \right) \right] \right. \right. \\ \left. \left. + \xi_z \frac{\partial}{\partial \xi} \left[\mu \left[R_r \frac{\partial U}{\partial R} + \xi_z \frac{\partial W}{\partial \xi} + \eta_z \frac{\partial W}{\partial \eta} \right] \right] \right. \right. \\ \left. \left. + \eta_z \frac{\partial}{\partial \eta} \left[\mu \left[R_r \frac{\partial U}{\partial R} + \xi_z \frac{\partial W}{\partial \xi} + \eta_z \frac{\partial W}{\partial \eta} \right] \right] \right. \right. \\ \left. \left. + \frac{1}{R} \left[2\mu \left(R_r \frac{\partial W}{\partial R} - \xi_\theta \frac{\partial V}{\partial \xi} - \eta_\theta \frac{\partial V}{\partial \eta} - \frac{W}{R} \right) \right] \right] \end{aligned}$$

Dropping the diffusion terms in the ξ direction, we get,

$$\begin{aligned} \text{R.H.S.} = & -R_r \frac{\partial P}{\partial R} + \frac{1}{Re} \left[\frac{\partial}{\partial R} \left(\frac{R_r}{J} \left[2\mu R_r \frac{\partial W}{\partial R} - \frac{2\mu}{3} \left[R_r \frac{\partial W}{\partial R} + \eta_\theta \frac{\partial V}{\partial \eta} + \eta_z \frac{\partial U}{\partial \eta} + \frac{W}{R} \right] \right) \right. \\ & + \eta_\theta \frac{\partial}{\partial \eta} \left[\mu \left(\eta_\theta \frac{\partial W}{\partial \eta} + R_r \frac{\partial V}{\partial R} - \frac{V}{R} \right) \right] + \eta_z \frac{\partial}{\partial \eta} \left[\mu \left[R_r \frac{\partial U}{\partial R} + \eta_z \frac{\partial W}{\partial \eta} \right] \right] \\ & \left. + \frac{1}{R} \left[2\mu \left(R_r \frac{\partial W}{\partial R} - \eta_\theta \frac{\partial V}{\partial \eta} - \frac{W}{R} \right) \right] \right] \end{aligned}$$

$$\begin{aligned} \text{R.H.S.} = & -R_r \frac{\partial P}{\partial R} + \frac{1}{Re} \left[\frac{\partial}{\partial R} \left(\frac{R_r}{J} \left[2\mu R_r \frac{\partial W}{\partial R} - \frac{2\mu}{3} \left[R_r \frac{\partial W}{\partial R} + \eta_\theta \frac{\partial V}{\partial \eta} + \eta_z \frac{\partial U}{\partial \eta} + \frac{W}{R} \right] \right) \right. \\ & + \frac{\partial}{\partial \eta} \left[\mu \frac{\eta_\theta}{J} \left(\eta_\theta \frac{\partial W}{\partial \eta} + R_r \frac{\partial V}{\partial R} - \frac{V}{R} \right) + \frac{\mu \eta_z}{J} \left(R_r \frac{\partial U}{\partial R} + \eta_z \frac{\partial W}{\partial \eta} \right) \right] \\ & \left. + \frac{1}{R} \left[2\mu \left(R_r \frac{\partial W}{\partial R} - \eta_\theta \frac{\partial V}{\partial \eta} - \frac{W}{R} \right) \right] \right] \end{aligned}$$

$$\begin{aligned} \text{R.H.S.} = & -R_r \frac{\partial P}{\partial R} + \frac{1}{Re} \left[\frac{\partial}{\partial R} \left(\frac{R_r}{J} \left[\frac{4}{3} \mu R_r \frac{\partial W}{\partial R} - \frac{2\mu}{3} \left[\eta_\theta \frac{\partial V}{\partial \eta} + \eta_z \frac{\partial U}{\partial \eta} + \frac{W}{R} \right] \right) \right. \\ & + \frac{\partial}{\partial \eta} \left[\frac{\mu}{J} \left(\eta_z^2 + \eta_\theta^2 \right) \frac{\partial W}{\partial \eta} + \frac{\mu \eta_\theta}{J} \left[R_r \frac{\partial V}{\partial R} - \frac{V}{R} \right] + \frac{\mu \eta_z}{J} R_r \frac{\partial U}{\partial R} \right] \\ & \left. + \frac{1}{R} \left[2\mu \left(R_r \frac{\partial W}{\partial R} - \eta_\theta \frac{\partial V}{\partial \eta} - \frac{W}{R} \right) \right] \right] \end{aligned}$$

So the complete transformed equation is

$$\begin{aligned} & \frac{\partial}{\partial \xi} \left(\frac{\xi_z}{J} \rho U W + \frac{\xi_\theta}{J} \rho V W \right) + \frac{\partial}{\partial \eta} \left(\frac{\eta_z}{J} \rho U W + \frac{\eta_\theta}{J} \rho V W \right) + \frac{\partial}{\partial R} \left(\frac{R_r}{J} \rho W^2 \right) + \frac{\rho}{R} (W^2 - V^2) \\ & - \rho \Omega^2 R - 2\rho \Omega V = -R_r \frac{\partial P}{\partial R} + \frac{1}{Re} \left[\frac{\partial}{\partial R} \left(\frac{R_r}{J} \left[\frac{4}{3} \mu R_r \frac{\partial W}{\partial R} - \frac{2\mu}{3} \left[\eta_\theta \frac{\partial V}{\partial \eta} + \eta_z \frac{\partial U}{\partial \eta} + \frac{W}{R} \right] \right) \right] \right. \\ & + \frac{\partial}{\partial \eta} \left[\frac{\mu}{J} \left(\eta_z^2 + \eta_\theta^2 \right) \frac{\partial W}{\partial \eta} + \frac{\mu \eta_\theta}{J} \left[R_r \frac{\partial V}{\partial R} - \frac{V}{R} \right] + \frac{\mu \eta_z}{J} R_r \frac{\partial U}{\partial R} \right] \\ & \left. + \frac{1}{R} \left[2\mu \left(R_r \frac{\partial W}{\partial R} - \eta_\theta \frac{\partial V}{\partial \eta} - \frac{W}{R} \right) \right] \right] \end{aligned}$$

$$\begin{aligned}
& \text{or} \\
& \frac{\partial}{\partial \xi} \left(\frac{\xi_z}{J} \rho U W + \frac{\xi_\theta}{J} \rho V W \right) + \frac{\partial}{\partial \eta} \left(\frac{\eta_z}{J} \rho U W + \frac{\eta_\theta}{J} \rho V W \right) + \frac{\partial}{\partial R} \left(\frac{R_r}{J} \rho W^2 \right) + \frac{\rho}{R} (W^2 - V^2) - \rho \Omega^2 R \\
& - 2\rho \Omega W = - \frac{\partial}{\partial P} \left(\frac{R_r}{J} P \right) + \frac{1}{R_\theta} \left[R_r \frac{\partial}{\partial R} \left(\frac{4}{3} \mu R_r \frac{\partial W}{\partial R} - \frac{2\mu}{3} \left(\eta_\theta \frac{\partial V}{\partial \eta} + \frac{W}{R} + \eta_z \frac{\partial U}{\partial \eta} \right) \right) \right. \\
& + \frac{\partial}{\partial \eta} \left[\frac{\mu}{J} (\eta_z^2 + \eta_\theta^2) \frac{\partial W}{\partial \eta} + \frac{\mu \eta_\theta}{J} \left[R_r \frac{\partial V}{\partial R} - \frac{V}{R} \right] + \mu \frac{\eta_z}{J} R_r \frac{\partial U}{\partial R} \right] \\
& \left. + \frac{1}{R} \left[2\mu \left(R_r \frac{\partial W}{\partial R} - \eta_\theta \frac{\partial V}{\partial \eta} - \frac{W}{R} \right) \right] \right]
\end{aligned}$$

Jacobian of E, F, G, C, P, Q, S

$$J_E = \frac{1}{J} \begin{bmatrix} 2\xi_z \rho U + \xi_\theta \rho V & \xi_\theta \rho U & 0 \\ \xi_z \rho V & \xi_z \rho U + 2\xi_\theta \rho V & 0 \\ \xi_z \rho W & \xi_\theta \rho W & \xi_z \rho U + \xi_\theta \rho V \end{bmatrix}$$

Jacobian of F

$$J_F = \frac{1}{J} \begin{bmatrix} 2\eta_z \rho U + \eta_\theta \rho V & \eta_\theta \rho U & 0 \\ \eta_z \rho V & \eta_z \rho U + 2\eta_\theta \rho V & 0 \\ \eta_z \rho W & \eta_\theta \rho W & \eta_z \rho U + \eta_\theta \rho V \end{bmatrix}$$

Jacobian of G

$$J_G = \frac{R_r}{J} \begin{bmatrix} \rho W & 0 & \rho U \\ 0 & \rho W & \rho V \\ 0 & 0 & 2\rho W \end{bmatrix}$$

Jacobian of C

$$J_C = \begin{bmatrix} \rho W/R & 0 & \rho V/R \\ 0 & 2\rho W/R + 2 & 2\rho(V/R + \Omega) \\ 0 & -2\rho(V/R + \Omega) & 2\rho W/R \end{bmatrix}$$

Jacobian of P

$$J_P = \frac{R_r}{J} \begin{bmatrix} \mu R_r \frac{\partial}{\partial R} & 0 & \mu \eta_z \frac{\partial}{\partial \eta} \\ 0 & \mu \left[R_r \frac{\partial}{\partial R} - \frac{1}{R} \right] & \mu \eta_\theta \frac{\partial}{\partial \eta} \\ \frac{-2\mu}{3} \eta_z \frac{\partial}{\partial \eta} & \frac{-2\mu}{2} \eta_\theta \frac{\partial}{\partial \eta} & \frac{4}{3} \mu R_r \frac{\partial}{\partial R} - \frac{2\mu}{3R} \end{bmatrix}$$

Jacobian of Q

$$J_Q = \begin{bmatrix} \mu \left(\frac{\eta_\theta^2 + \eta_z^2}{J} \right) \frac{\partial}{\partial \eta} + \frac{\mu}{3} \frac{\eta_z^2}{J} \frac{\partial}{\partial \eta} & \frac{\mu}{3} \frac{\eta_z}{J} \eta_\theta \frac{\partial}{\partial \eta} & -\frac{2}{3} \frac{\eta_z}{J} \left(R_r \frac{\partial}{\partial R} + \frac{1}{R} \right) \\ \frac{\mu}{3} \frac{\eta_\theta \eta_z}{J} \frac{\partial}{\partial \eta} & \mu \left(\frac{\eta_\theta^2 + \eta_z^2}{J} \right) \frac{\partial}{\partial \eta} + \frac{\mu}{3} \frac{\eta_\theta^2}{J} \frac{\partial}{\partial \eta} & -\frac{2}{3} \mu \frac{\eta_\theta}{J} \left(R_r \frac{\partial}{\partial R} - \frac{2}{R} \right) \\ \mu \frac{\eta_z}{J} R_r \frac{\partial}{\partial R} & \mu \frac{\eta_\theta}{J} \left[R_r \frac{\partial}{\partial R} - \frac{1}{R} \right] & \mu \left(\frac{\eta_\theta^2 + \eta_z^2}{J} \right) \frac{\partial}{\partial \eta} \end{bmatrix}$$

Jacobian of S

$$J_S = \begin{bmatrix} \frac{\mu}{R} R_r \frac{\partial}{\partial R} & 0 & \frac{\mu}{R} \eta_z \frac{\partial}{\partial \eta} \\ 0 & \frac{2\mu}{R} \left[R_r \frac{\partial}{\partial R} - \frac{1}{R} \right] & \frac{2\mu}{R} \eta_\theta \frac{\partial}{\partial \eta} \\ 0 & -\frac{2\mu}{R} \eta_\theta \frac{\partial}{\partial \eta} & \frac{2\mu}{R} R_r \frac{\partial}{\partial R} - \frac{1}{R} \end{bmatrix}$$

APPENDIX 2

Literature Survey on the Effects of Curvature and Rotation on Turbulence Structure

In this section a literature survey on experimental and analytical investigation of the curvature and rotation effects on turbulence is carried out.

Experimental results provide information on the physical behavior of the turbulent flows to enable modelling the effects of the different strains such as mean strains, curvature effects, rotation effects, etc. The triple velocity correlations, pressure-velocity correlations, dissipation which appear in the Reynolds stress equation, are difficult to measure and, hence, the modeling is more or less empirical and is based generally on very restrictive assumptions. For example, the turbulence models are often based on the homogeneous fluid properties, local isotropy of dissipative scales, high Reynolds numbers which lead to relatively simple models. On the other hand, experimental work provide results that can be used to check different turbulence models. Nevertheless, some of the experiments do not provide sufficient information to check all the models in detail. In the past few years, it seems that a great effort has been made to provide experimental data including all the Reynolds stress tensor terms. Most of the data available is for simple two dimensional shear flows (free shear flows, boundary layers, jets, wakes, ducts). For the complex flows (following the definition of Bradshaw (1977) for complex flows) which are the most common in engineering practice, very little data and few models are available.

In this section, more emphasis is given to the effect of rotation which is the principal effect we are interested in.

Curvature Effects

Experimental Data

Castro and Bradshaw (1976) have carried out extensive one-point measurements in a highly curved mixing layer to determine the effects of streamline curvature on a shear layer. The principal effect is to diminish the Reynolds stress tensor components when the angular momentum of the mean flow increases with radius of curvature and to increase these quantities in the opposite situation. The most spectacular feature of the measurements is that the components of the Reynolds stress tensor after decreasing in the highly stabilizing curvature region, rise rapidly and overshoot the plane-layer value farther downstream before finally decreasing. This indicates the inadequacy in current modeling for shear layers such as the use of the shear layer thickness to provide a length scale, the rotational invariance of turbulence models based on second order transport equations, and the gradient diffusion hypothesis for turbulent transport.

Changes in turbulence properties can occur even with small curvatures as can be seen in the experiments of Hoffmann and Bradshaw (1978) on a turbulent boundary layer with a mild longitudinal curvature, and of Hunt and Joubert (1979) in duct flow. Data are also reported by So and Mellor (1975) who show that Reynolds stress increases and three-dimensional vortices exist over a concave surface. The experiments of Margolis (1963) deal with the unstable effects in a curved mixing layer. The latest paper by Nakano et al. (1981) covers the effects of stable and unstable freestream on a turbulent flow over a concave surface, where different shear flows are provided at the inlet to the curved section. Three-dimensional longitudinal

vortices are found. In an unstable free stream, turbulent intensities in the boundary layer as well as in the free stream are increased. Alcaraz (1977) studied the wall jet developing on a constant-radius convex curved surface. The flow was nearly two-dimensional, but the curvature was large enough to produce measurable effects on turbulence.

Analysis

The effect of stabilizing or destabilizing forces on the turbulent motion of homogeneous fluids in flows along curved surfaces was first discussed by Prandtl (1930). Early experiments gave evidence that the intensity of turbulence increases on concave surfaces and decreases on convex surfaces. Similar effects occur, when the gravity field acts on a flow of variable density. Görtler (1959) has pointed out the analogy between the two effects. Bradshaw (1968) proposed a formal algebraic analogy between meteorological parameters, such as Richardson number and the parameters describing the effect of curvature or rotation on turbulent flows. Semi-quantitative use of the analogy shows that the effects of curvature are appreciable if the shear layer thickness exceeds roughly $1/300$ of the radius of curvature. The main result of the paper is the introduction of the Richardson numbers for streamline curvature and rotation which represent the ratio of the "buoyant" production to inertia production. Bradshaw also proposed a form of the Monin-Oboukhov formula for the change of mixing length with Richardson number for curved flows. The development of multi-equation models for curved flow began nearly 1975 with Mellor who in fact used the same stress closure approximations for buoyant flow and curved flow to produce a modifying function for the

eddy viscosity. Irwin and Smith (1975) simplified the stress-closure of Launder et al. (1975) to calculate the development of boundary layers and wall jets on curved surfaces. The most important result was that the observed curvature effects could be accounted for by the relatively small production terms appearing in the individual Reynolds stress equations. Launder et al. (1977) proposed a two-equation model (k- ϵ). The energy production rate due to curvature appears in exact form in the energy equation, but the curvature effect is modeled empirically in the dissipation equation. Gibson (1978) developed an algebraic Reynolds stress model, following the idea that effects of curvature on heat transfer could only be accounted for by modelling the Reynolds-stress and heat-flux equations. The model is derived from that developed for the buoyancy affected turbulence. The influence of the wall is introduced in the modeling of the fluctuating pressure. It is shown that the effects of streamline curvature on heat transfer are probably significantly less than on the shear stress. That is an important result which suggests that the use of a constant turbulent Prandtl number in prediction methods may provide misleading estimates of the heat transfer from curved surfaces. The algebraic Reynolds stress model may be coupled with a one equation scheme (k) or two-equation (k- ϵ) models to provide a length scale. Recently Townsend (1980) introduced the rapid-distortion approximation to predict the streamwise variation of \overline{uv}/q^2 , considering that the complex distortion involves taking account for the history of the distortion. Two remarks are to be made. Firstly, this approach may not be suitable for mild curvature surfaces, where the time scales of turbulence motion and distortion can be of the same order. Secondly, this method predicts only stress ratios, and if it were to form part of a calculation scheme, other equations would be needed to determine the intensities. More recently, Gibson and Rodi (1981) have proposed a full

Reynolds stress model for two-dimensional curved flows and for high Reynolds numbers. The modelling is principally based on Launder et al. (1975) model, using the simple gradient diffusion hypothesis for the triple velocity correlation due to Daly and Harlow (1970). In adapting the pressure-strain correlation to curved flow, the mean shear production as well as the extra strain due to curvature are included, though the effects of curvature are implicitly introduced in the modeling. The modeled ϵ equation, in the form originally proposed by Hanjalic and Launder (1972) appears to be quite adequate, only a logical change has been done in that equation. The energy production due to mean shear in a simple flow is replaced by the total (shear and curvature) production. However, recently the performance of the modeled equation for ϵ has been questioned [Launder and Morse (1979), Hanjalic and Launder (1978)] for complex flows. So, one of the most updated works to be done should be the modeling of the exact equation. Particularly when curvature and rotation effects are present. We may mention the latest works of Gibson, Jones, Younis (1981) on curved wall boundary layer and, Gibson and Younis (1981) on curved wall jet more particularly on a convex surface [Alcaraz (1977)]. The only difference in modeling with the previous work of Gibson and Rodi (1981) is in the way of how the pressure strain correlation is modeled. The proposed modification for near-wall effect by Launder et al. (1975) is used. All these calculations are part of a program motivated by the requirement for a general prediction procedure for complex shear flows with density stratification, rotation and streamline curvature.

Rotation Effects

Experimental Data

It was pointed out by Johnston (1970), that there are two basic effects of rotation. If components of the coriolis acceleration is parallel to the surface on which the layers are growing, secondary flows will tend to develop in the mean flow field of the layers. If a component of the coriolis acceleration is perpendicular to a solid surface, some stabilizing and destabilizing effects are observed in the turbulence structure itself. Both effects are believed to be important in the flow fields of centrifugal impellers.

The experimental data available may be classified in two categories.

1. Free shear flows in rotating frames (e.g., wakes), and
2. Wall shear flows.

In the case of free shear flows, only the experiment of Raj and Lakshminarayana (1975) is known to us. These authors give a detailed measurement of the wake characteristics behind a rotor. The results of Ravindranath and Lakshminarayana (1980) are also available.

In the case of wall shear flows, one may class the different experiments available in three categories:

1. Rotating Cylinders or Pipes
2. Centrifugal Turbomachines
3. Axial Turbomachines

1. Rotating Cylinders in Axial Flow

Almost all the experiments designed in this case are nearly the same.

We may mention here the works of Bissonnette and Mellor (1970), and

Lohmann (1973). In each of these experiments the mean properties and the six components of the Reynolds tensors are measured, but the major effects due to the rotation occur very near the wall and the turbulent quantities are not measured in this part of the boundary layer.

Arzoumanian et al. (1981) has provided data on an axially rotated cylinder with special emphasis in the region very close to the moving wall, nevertheless, only the following turbulent quantities are measured: $\overline{u'^2}$, $\overline{w'^2}$, $\overline{u'w'}$. The turbulent stresses $\overline{u'v'}$ and $\overline{w'v'}$ are derived by integrating the corresponding momentum equations from mean velocity measurements. Nakamura et al. (1981), in their study of a three-dimensional turbulent boundary layer on a spinning thin cylinder in an axial flow, have given some results on the mean properties. A universal law for velocity distribution is also derived. The experiment on the three dimensional boundary layer developing in an axially rotating pipe of Murakami et al. (1981) show that the flow is affected by two counter effects. One is a destabilizing effect due to an increase of the relative velocity at the wall caused by the pipe rotation, and the other is a stabilizing effect due to the suppression of turbulence by the centrifugal force. The dominant effect depends on the Reynolds number and the rotational speed.

2. Models of Centrifugal Turbomachines

The effects of the coriolis forces in such machines are of great importance. The experiments of I-Man Moon (1964) provide some results on the mean quantities as well as on the following components of the Reynolds stress tensor: $\overline{u'^2}$, $\overline{v'^2}$, $\overline{u'v'}$ for a rotating speed of 165 rpm and $0.48 \leq R_0 \leq 1.92$. Moore (1973) carried out similar measurements but provided

only mean velocity profiles. Johnston et al. (1972) in their experiment on fully developed turbulent flow in a channel, which is rotating about a spanwise axis, observed three stability related phenomena explained in this paper. They pointed out the Richardson number is an appropriate local stability parameter. For example, local effects of rotational stabilization, such as reduction of the turbulent stress in wall layers, can be related to the local Richardson number in a simple way. In this experiment, the authors also give some quantitative data on mean properties. The paper of Koyama et al. (1979) on "The Turbulence Structure and Three Dimensionality of a Rotating Two Dimensional Turbulent Boundary Layer" is one of the latest results available. This paper has not been surveyed at this time. We may also introduce the partial results of Bertoglio et al. (1980) in a centrifugal testing machine which give some information on the flow in actual impeller.

3. Model of Axial Turbomachines

For such cases, only few results are known, in fact the only available data are the ones provided at The Pennsylvania State University--the experiment of Lakshminarayana et al. (1972) on the turbulent boundary layer on a rotating helical blade. However, no turbulent measurements are included in these results. The more complete experiment was Anand and Lakshminarayana's (1975, 1978) on the four bladed rotating helical channel. Some results on turbulence quantities show that the radial component of turbulence intensities is higher than the streamwise component due to the effect of rotation. Moreover, the flow near the annulus wall is found to be highly complex. The turbulent shear stress measurements show that in three dimensional rotating turbulent boundary layers, all three correlations are of the same order of magnitude inside the boundary layer. A deviation is found between the stress

tensor and the strain tensor, that is one of the most important features in three-dimensional flows and represents the anisotropy of the turbulence in such cases.

Analysis

Bradshaw (1969) carried out a simple analysis for both curvature effects and rotation effects and pointed out that the same arguments could be applied to shear layers in rotating fluids and curved flows. The author introduced the gradient Richardson number, the flux and stress Richardson number by analogy with buoyancy analysis. A more detailed qualitative analysis has been carried out by Johnston et al. (1972) for the case of a rotating boundary layer. In their study, they focused attention on the production terms which appear in the Reynolds stress equations and which are due to the interaction by the mean flow and due to coriolis effects, explicitly. In summary, this examination of the production terms lead to conclude that in wall layers the sign and the magnitude of rotation effects might be controlled by a local dimensionless parameter. This parameter may be related to the gradient Richardson number proposed by Bradshaw and is very useful to characterize the stability or instability of the flow submitted to a rotation. It appears that the first "theoretical" investigations and prediction procedures accounting for all the effects of the flow situation, namely three-dimensionality and turbulence, are quite new. In fact the first attempts to calculate three dimensional boundary layer are based on integral methods such as Moore (1973), Lakshminarayana et al. (1981). The first differential calculations seem to be those of Majumdar et al. (1977) and Sharma (1977).

In the former case, the authors are solving the three-dimensional boundary layer with the method of Patankar-Spalding (1972), which is a marching integration technique for three-dimensional boundary layer problems. The turbulence model which is used in this paper is the well known $k-\epsilon$ model without any modifications for the rotation effects. In the latter case, e.g. Sharma's paper, the calculation over an axially spinning cylinder is performed. The problem is two-dimensional and solved with the two-dimensional marching procedure of Patankar-Spalding (1970). The $k-\epsilon$ model is used to calculate the boundary layer up to the wall. An additional term is included in the transport equation for ϵ to account for the curvature effect on the dissipation rate. This term is seen as a correction to the "dissipation" of dissipation rate ϵ by the Richardson number based on the turbulent time scale k/ϵ . Nevertheless, this kind of model cannot account for the non-isotropy of the stress tensor. Moreover, no correction for the rotation effects are introduced. In fact, these effects are not very important for the calculation of flow on spinning cylinder. On the problem of the rotating cylinder, an approach similar to Sharma's is due to Spitz (1980) who solved the same momentum equations as Sharma with the same numerical procedure. In this work an attempt is made to include the non-isotropy of the Reynolds stress tensor by taking account for two eddy viscosity factors which represent the difference between the two principal directions. The turbulence model is based on the mixing length hypothesis. We may also mention the work of Cousteix and Aupoil (1979) who made the same assumptions but used a $k-\epsilon$ model. But in each of these works no rotation effects were included.

One of the first analysis of the rotation effects on the turbulence quantities has been carried out by Raj and Lakshminarayana (1975) and Raj (1975), who gave the exact equation in generalized tensor notations and analyzed the turbulent processes in the wake of the rotor blade, but no calculations were carried out. Lakshminarayana and Reynolds (1979) carried out a qualitative analysis of the effects of rotation on turbulence in the near wake of a rotor. This analysis indicates that the rotation has substantial effects on the structure of turbulence. Such as radial component of intensities is higher than the axial and tangential in the near wake and decay more rapidly than the others. The radial components of the stresses are generally higher than those of a corresponding non-rotating case.

Another analysis based on spectral calculus has been carried out by Bertoglio et al. and Bertoglio (1980) to study the effects of the rotation on an homogeneous turbulent field. The effects of stabilizing and destabilizing due to coriolis forces are observed, but this kind of approach does not account for the non-linear and inhomogeneous terms in the computation. Nevertheless, some important results show that the pressure-strain correlation in rotating frames may have to be modeled carefully. Another fact is that the use of isotropic functions when modeling may be inadequate, and some parameters, like the direction of the force, have to be taken into account.

The only complete calculation available, which takes into account the rotation effects, is the one performed by Howard et al. (1980). These authors, following the work of Majumdar et al. (1977), used a modified procedure based on the partially-parabolic method of Majumdar and Spalding (1977). They solve the three-dimensional boundary layer equations within a rotating frame. The turbulence model is based on the k- ϵ model. Three

modifications to the basic k-ε model are tested which include effects of Coriolis force on the turbulent energy and dissipation rate. The first model is based on the work of Wilcox and Chambers (1977) and take account of the Coriolis effects in both the k and ε equations assuming that the kinetic energy is proportional to $\overline{u'^2}$. The second and third models are based on a study of curved boundary layers by Launder et al. (1977), where the k equation is maintained in its usual form and where the Coriolis effect is introduced through the ε equation. Two forms of the Richardson number are considered. Their conclusion is that the Wilcox-Chambers model give the most satisfactory prediction, and they point out the need for inclusion of a Coriolis model for turbulence modification. Finally, the approach of Hah and Lakshminarayana (1980) and Hah (1981) who introduce an algebraic Reynolds stress model coupled with a k-ε model which, though the convection and diffusion are not included, take account for rotation and curvature effects.

Comments

The review of the different paper point out three main features:

1. Only few calculations are available for the calculation of the three-dimensional boundary layer in rotating frames.
2. No complete Reynolds stress model is available for rotating turbulent flows. Very few attempts have been made to account for the rotation effects in the k-ε model, but none are really based on a logical analysis. In fact, the most up to date results in modeling are those of Raj (1975) and Hah and Lakshminarayana (1980). The major effort, then, should be given to the analysis of the dissipation rate equation and to the Reynolds stress equations.

3. Detailed measurements providing information on the effects of both the Rossby and the Richardson number on turbulence are not very numerous. So, every new result would be of great interest, particularly if the rotation effect can be isolated from the other effects.

LIST OF FIGURES

- Figure 1. Blade to blade distribution of axial (WZ), tangential (WT), and radial (WR) velocities at $Z = 0.26$, $R = 0.918$
- Figure 2. Blade to blade distribution of axial (WZ), tangential (WT), and radial (WR) velocities at $Z = 0.5$, $R = 0.918$
- Figure 3. Blade to blade distribution of axial (WZ), tangential (WT), and radial (WR) velocities at $Z = 0.73$, $R = 0.918$
- Figure 4. Blade to blade distribution of axial (WZ), tangential (WT), and radial (WR) velocities at $Z = 0.97$, $R = 0.918$
- Figure 5. Blade to blade distribution of stagnation (P_{TOTAL}) and static (P_{STATIC}) pressure at $Z = 0.26$, $R = 0.918$
- Figure 6. Blade to blade distribution of stagnation (P_{TOTAL}) and static (P_{STATIC}) pressure at $Z = 0.5$, $R = 0.918$
- Figure 7. Blade to blade distribution of stagnation (P_{TOTAL}) and static (P_{STATIC}) pressure at $Z = 0.73$, $R = 0.918$
- Figure 8. Blade to blade distribution of stagnation (P_{TOTAL}) and static (P_{STATIC}) pressure at $Z = 0.97$, $R = 0.918$
- Figure 9. Axial (WZ), tangential (WT), and radial (WR) velocity profiles at $Z = 1.049$, $R = 0.587$
- Figure 10. Axial (WZ), tangential (WT), and radial (WR) velocity profiles at $Z = 1.061$, $R = 0.67$
- Figure 11. Axial (WZ), tangential (WT), and radial (WR) velocity profiles at $Z = 1.069$, $R = 0.75$
- Figure 12. Axial (WZ), tangential (WT), and radial (WR) velocity profiles at $Z = 1.077$, $R = 0.832$
- Figure 13. Axial (WZ), tangential (WT), and radial (WR) velocity profiles at $Z = 1.085$, $R = 0.918$
- Figure 14. Stagnation (P_{TOTAL}) and static (P_{STATIC}) pressure profiles at $Z = 1.049$, $R = 0.587$
- Figure 15. Stagnation (P_{TOTAL}) and static (P_{STATIC}) pressure profiles at $Z = 1.061$, $R = 0.67$

Figure 16. Stagnation (P_{TOTAL}) and static (P_{STATIC}) pressure profiles at
 $Z = 1.069$, $R = 0.75$

Figure 17. Stagnation (P_{TOTAL}) and static (P_{STATIC}) pressure profiles at
 $Z = 1.077$, $R = 0.832$

Figure 18. Stagnation (P_{TOTAL}) and static (P_{STATIC}) pressure profiles at
 $Z = 1.049$, $R = 0.918$

ORIGINAL PAGE IS
OF POOR QUALITY

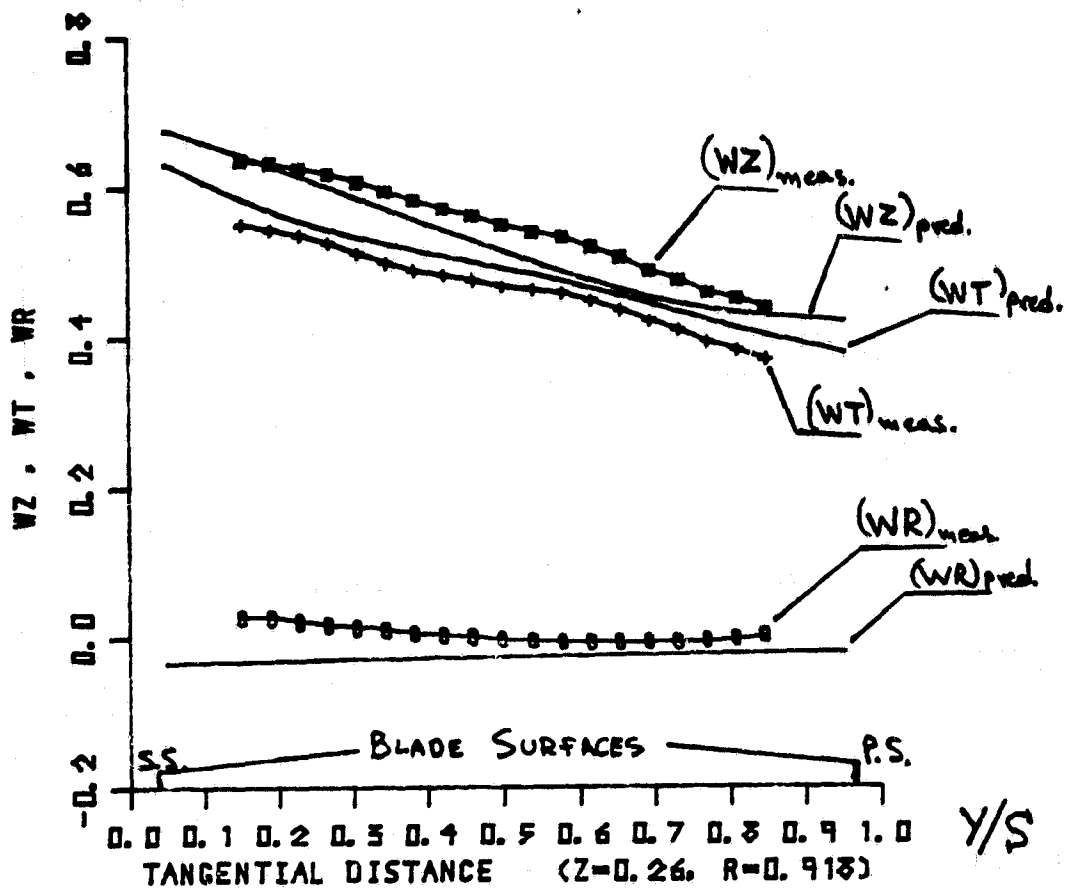


Figure 1. Blade to blade distribution of axial (WZ), tangential (WT), and radial (WR) velocities at $Z = 0.26$, $R = 0.918$

ORIGINAL PAGE IS
OF POOR QUALITY

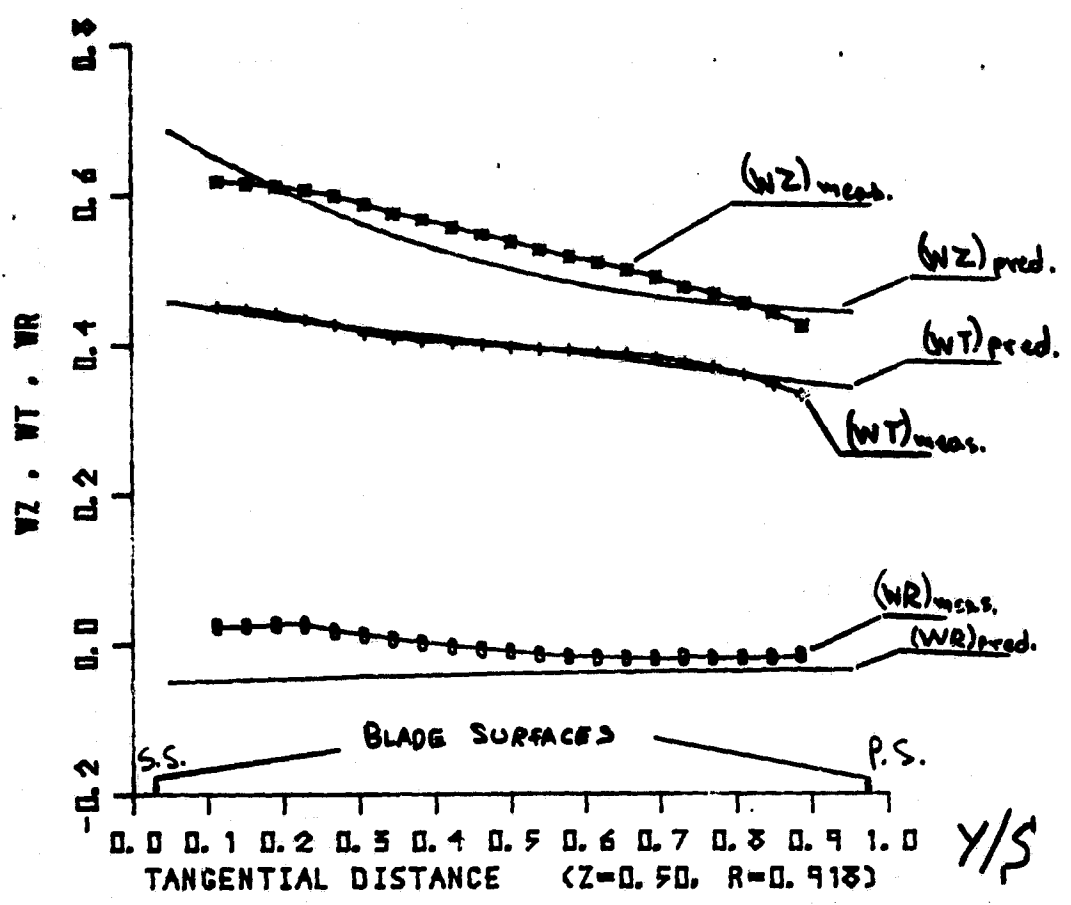


Figure 2. Blade to blade distribution of axial (WZ), tangential (WT), and radial (WR) velocities at $Z = 0.5$, $R = 0.918$

ORIGINAL PAGE IS
OF POOR QUALITY

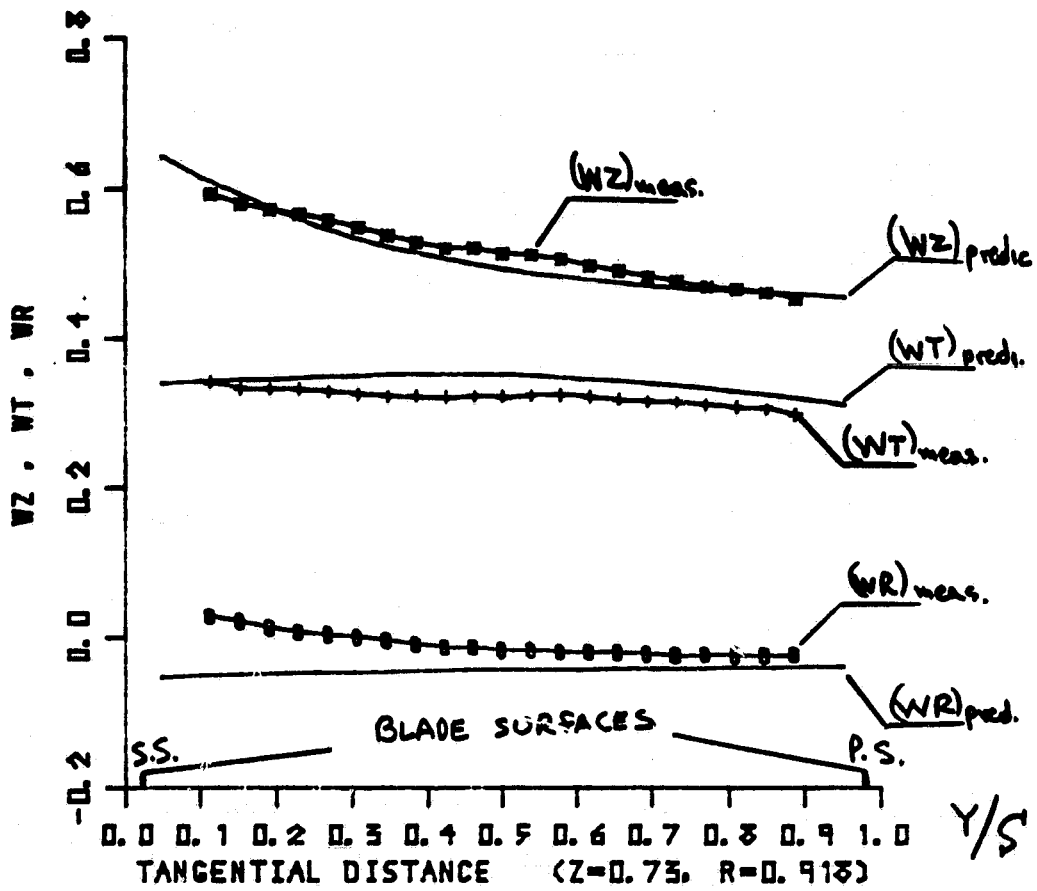


Figure 3. Blade to blade distribution of axial (WZ), tangential (WT), and radial (WR) velocities at $Z = 0.73$, $R = 0.918$

ORIGINAL PAGE IS
OF POOR QUALITY

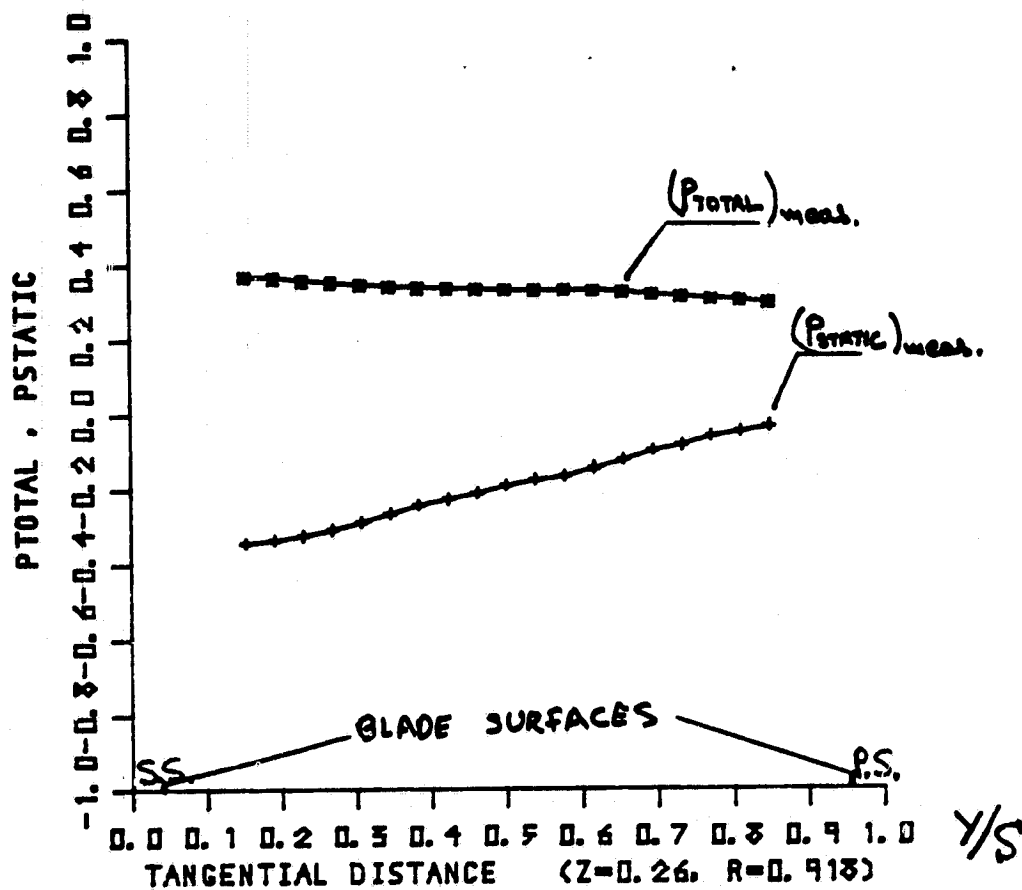


Figure 5. Blade to blade distribution of stagnation (P_{TOTAL}) and static (P_{STATIC}) pressure at $Z = 0.26$, $R = 0.918$

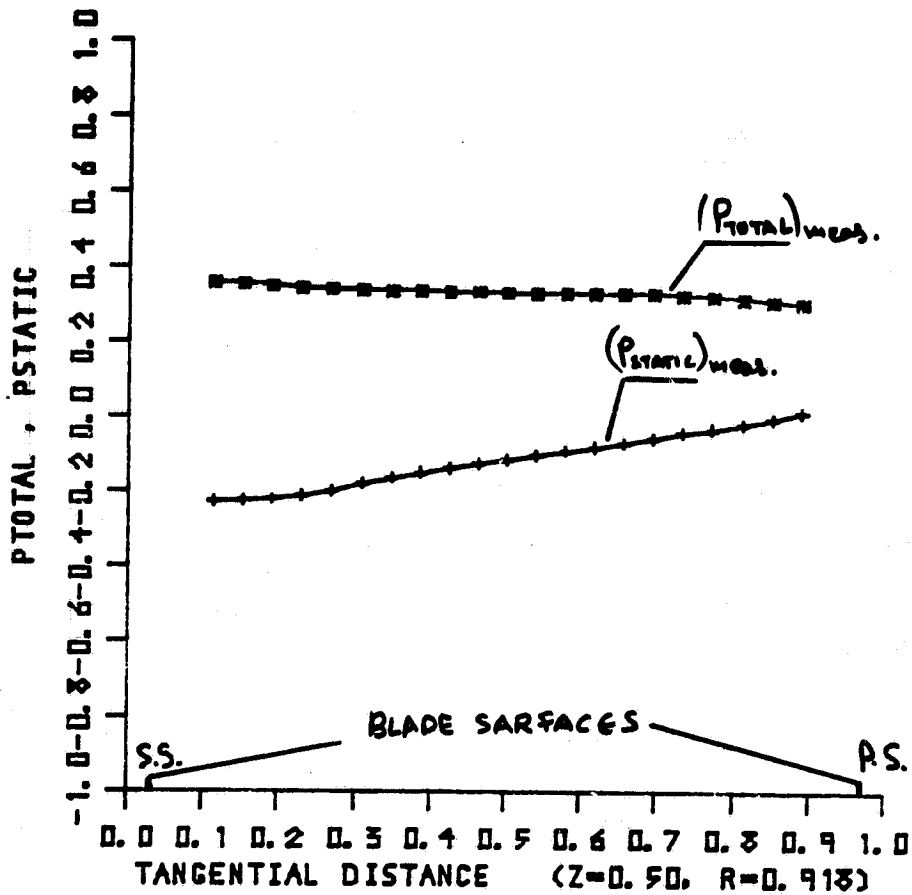
ORIGINAL PAGE IS
OF POOR QUALITY

Figure 6. Blade to blade distribution of stagnation (P_{TOTAL}) and static (P_{STATIC}) pressure at $Z = 0.5$, $R = 0.918$

ORIGINAL PAGE IS OF POOR QUALITY.

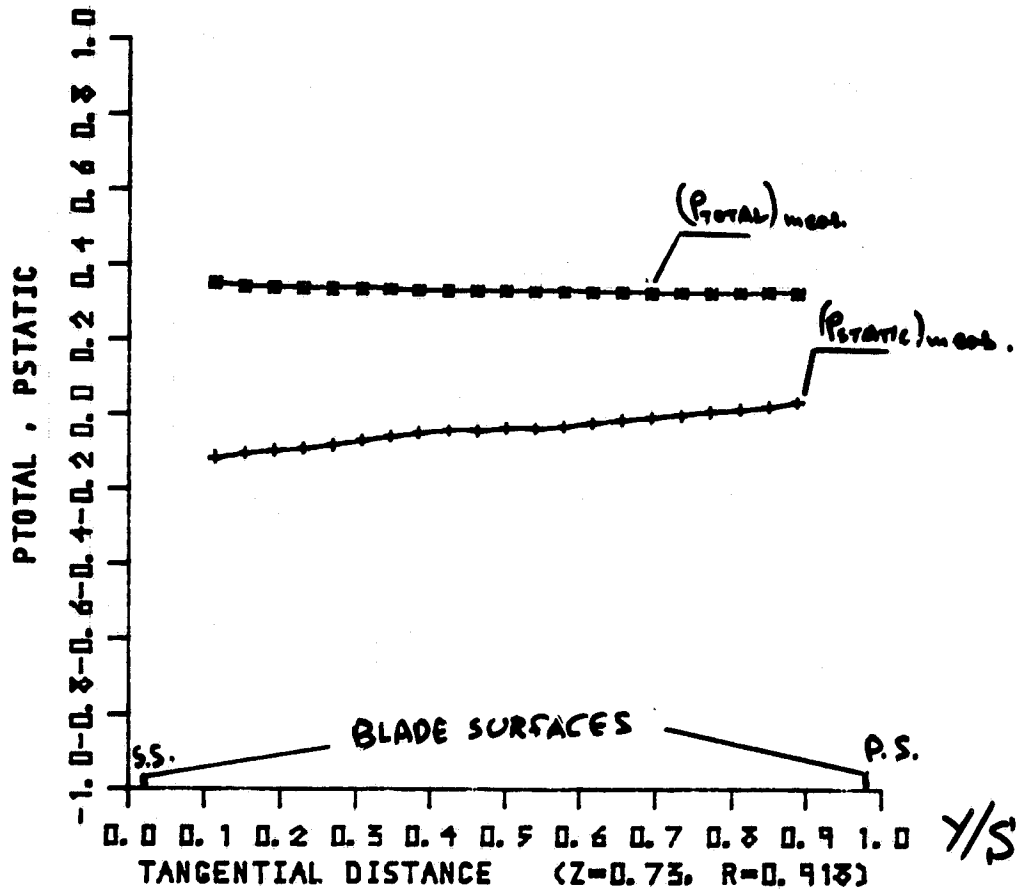


Figure 7. Blade to blade distribution of stagnation (P_{TOTAL}) and static (P_{STATIC}) pressure at Z = 0.73, R = 0.918

ORIGINAL PAGE IS
OF POOR QUALITY

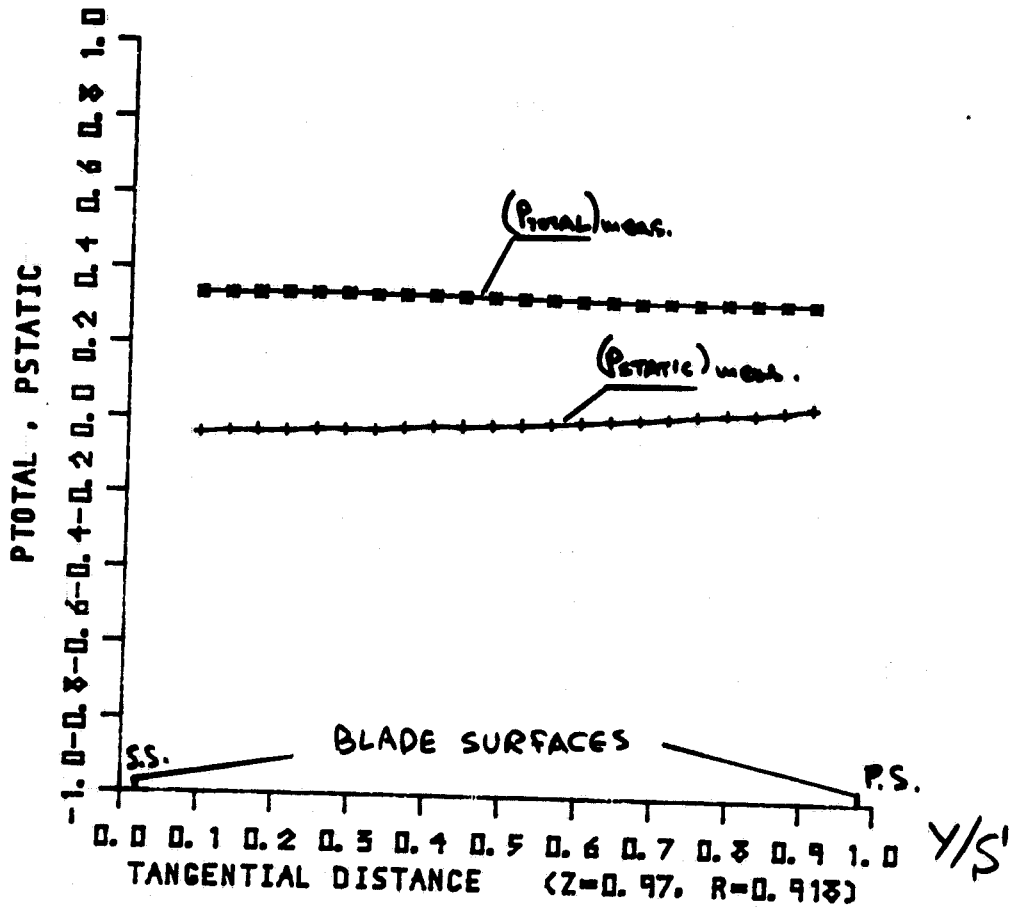


Figure 8. Blade to blade distribution of stagnation (P_{TOTAL}) and static (P_{STATIC}) pressure at $Z = 0.97$, $R = 0.913$

ORIGINAL PAGE IS
OF POOR QUALITY

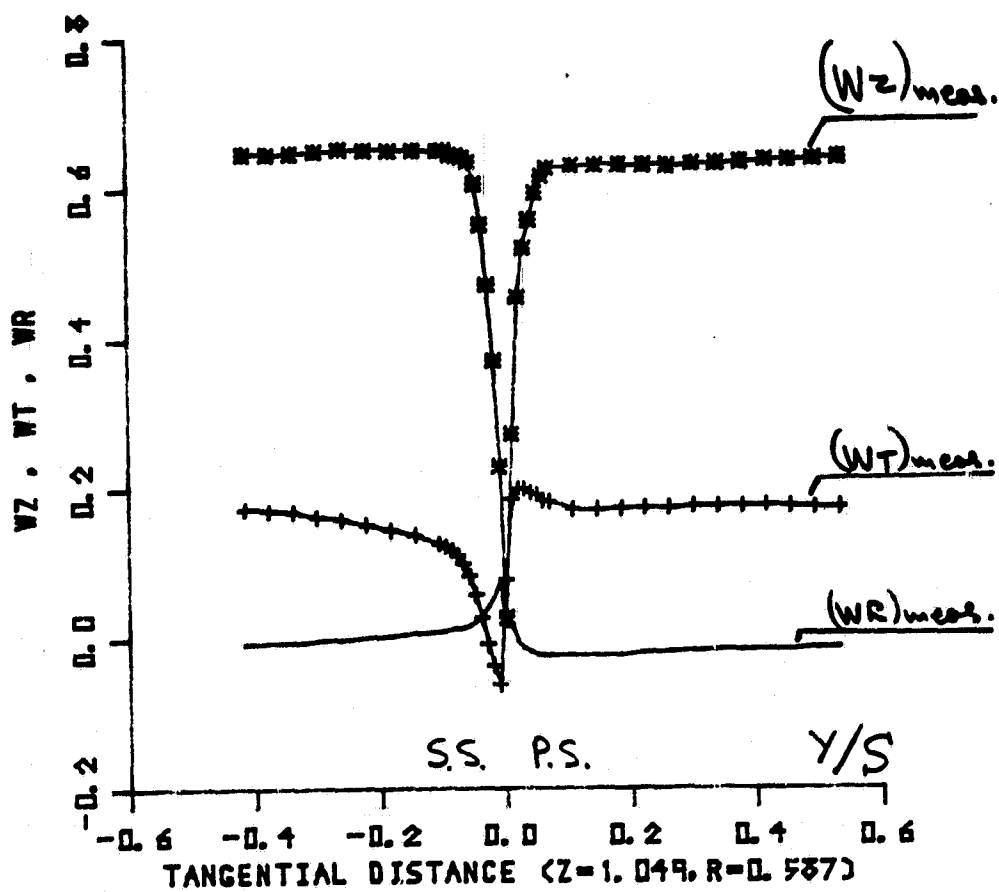


Figure 9. Axial (WZ), tangential (WT), and radial (WR) velocity profiles at $Z = 1.049$, $R = 0.587$

ORIGINAL PAGE IS
OF POOR QUALITY

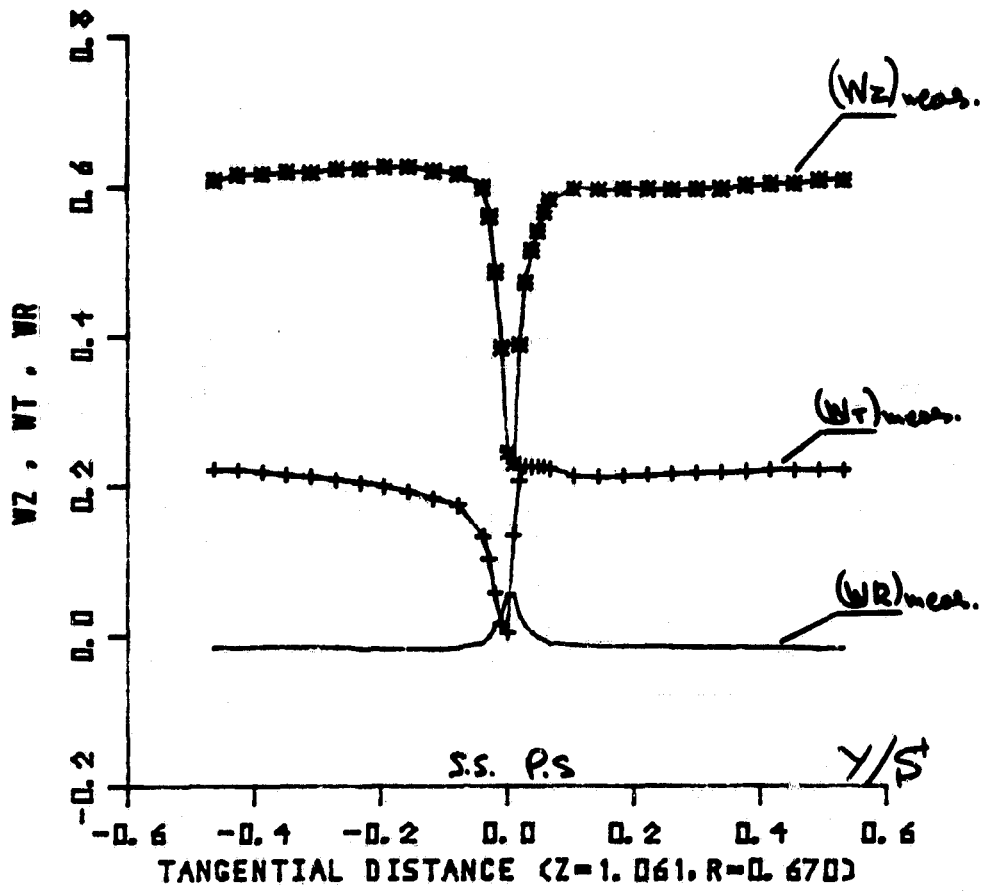


Figure 10. Axial (WZ), tangential (WT), and radial (WR) velocity profiles at $Z = 1.061$, $R = 0.67$

ORIGINAL PAGE IS
OF POOR QUALITY

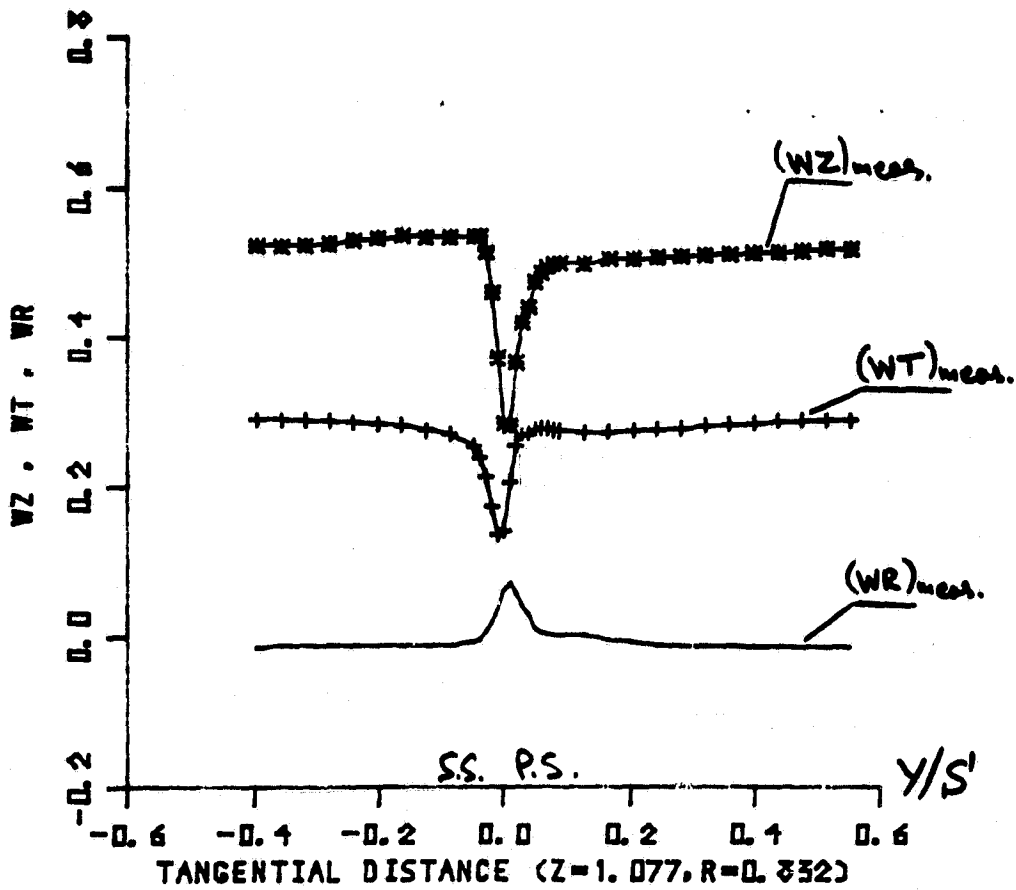


Figure 12. Axial (WZ), tangential (WT), and radial (WR) velocity profiles at $Z = 1.077$, $R = 0.832$

ORIGINAL PAGE IS
OF POOR QUALITY

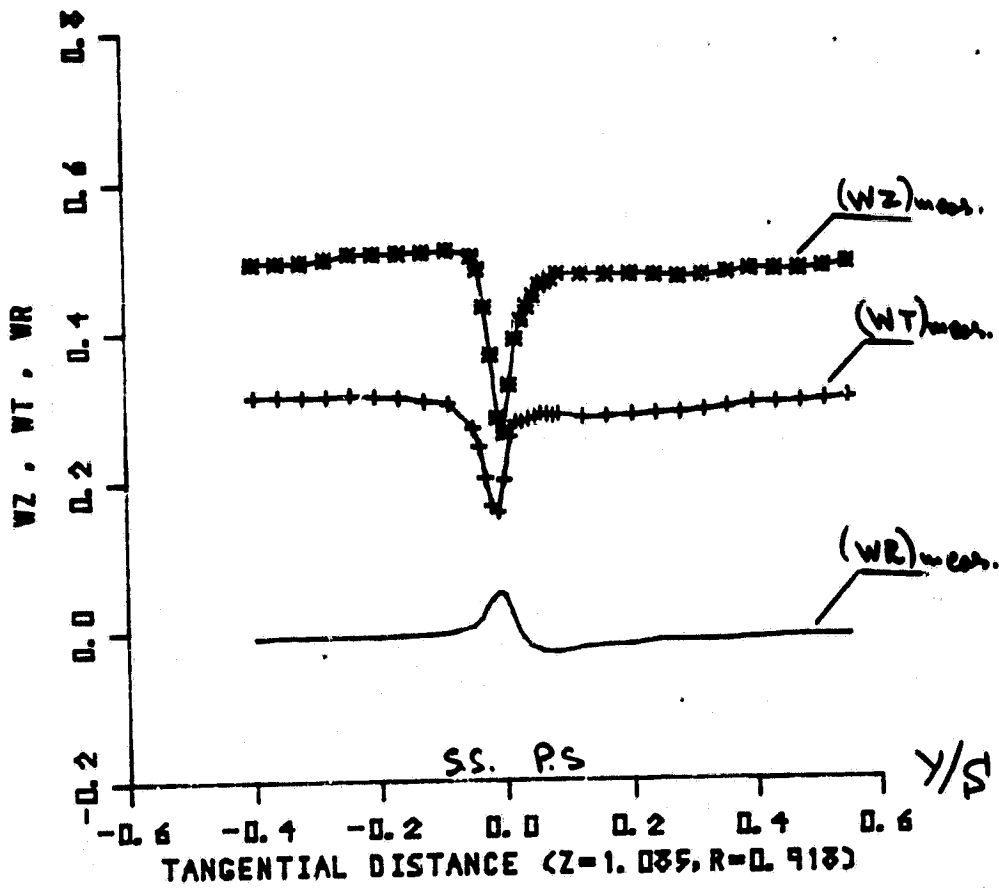


Figure 13. Axial (WZ), tangential (WT), and radial (WR) velocity profiles at $Z = 1.085$, $R = 0.918$

ORIGINAL PAGE IS
OF POOR QUALITY

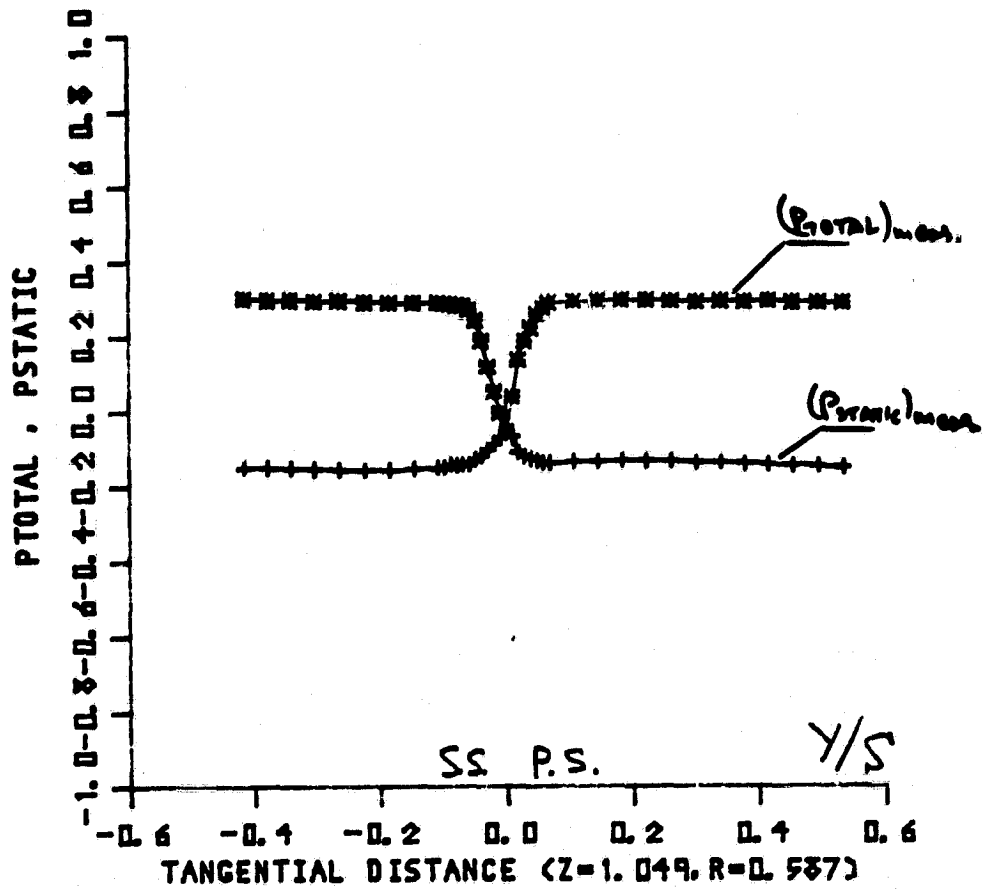


Figure 14. Stagnation (P_{TOTAL}) and static (P_{STATIC}) pressure profiles at $Z = 1.049$, $R = 0.587$

ORIGINAL PAGE IS
OF POOR QUALITY

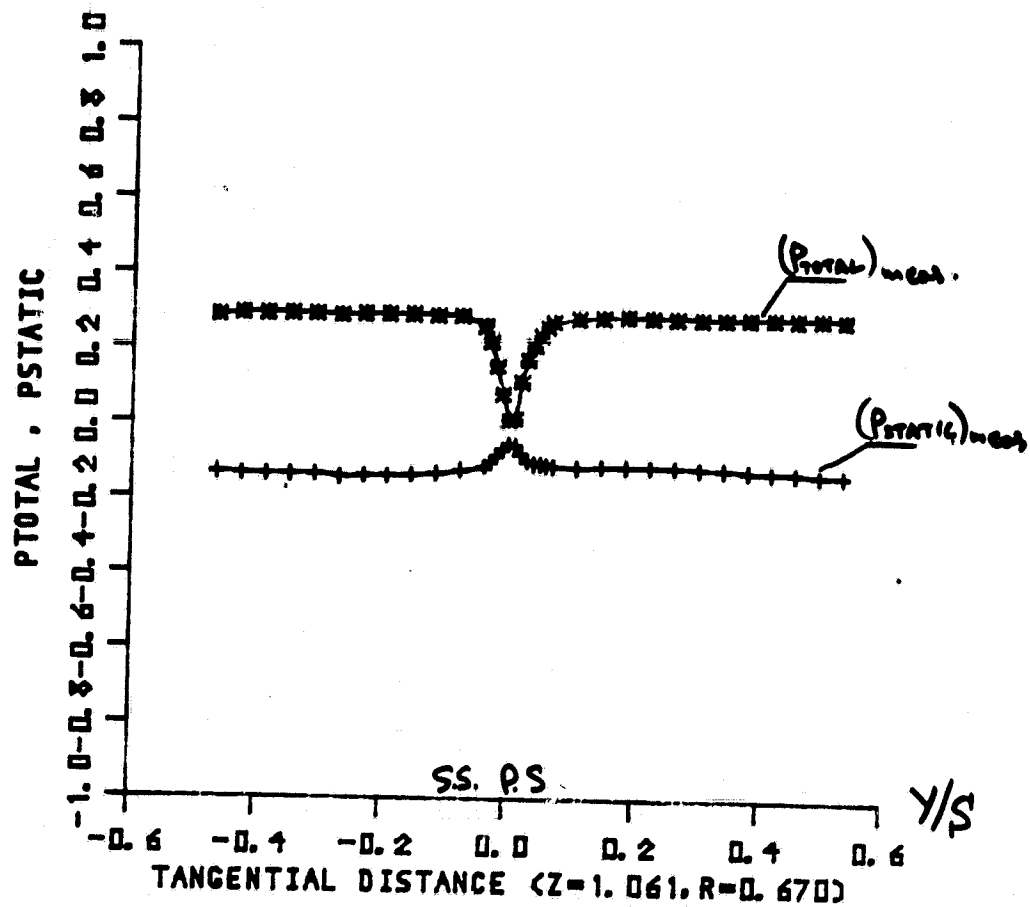


Figure 15. Stagnation (P_{TOTAL}) and static (P_{STATIC}) pressure profiles at $Z = 1.061$, $R = 0.67$

ORIGINAL PAGE IS
OF POOR QUALITY

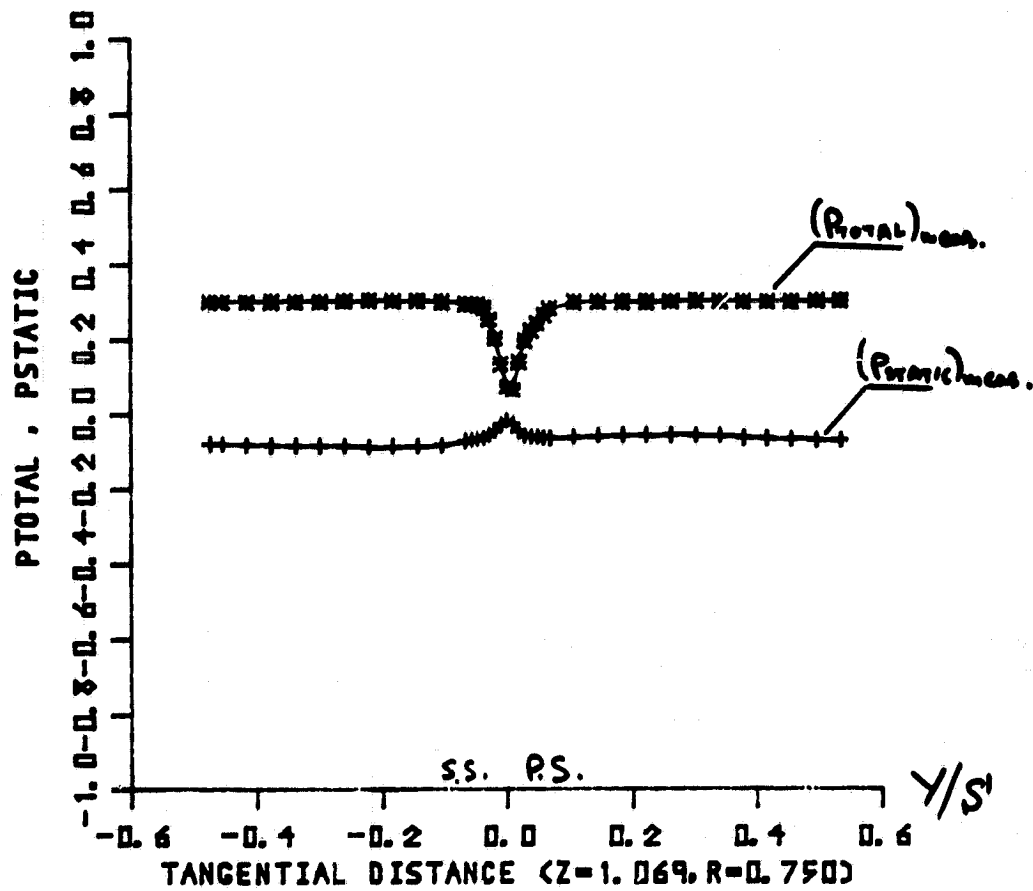


Figure 16. Stagnation (P_{TOTAL}) and static (P_{STATIC}) pressure profiles at $Z = 1.069$, $R = 0.75$

ORIGINAL PAGE IS
OF POOR QUALITY

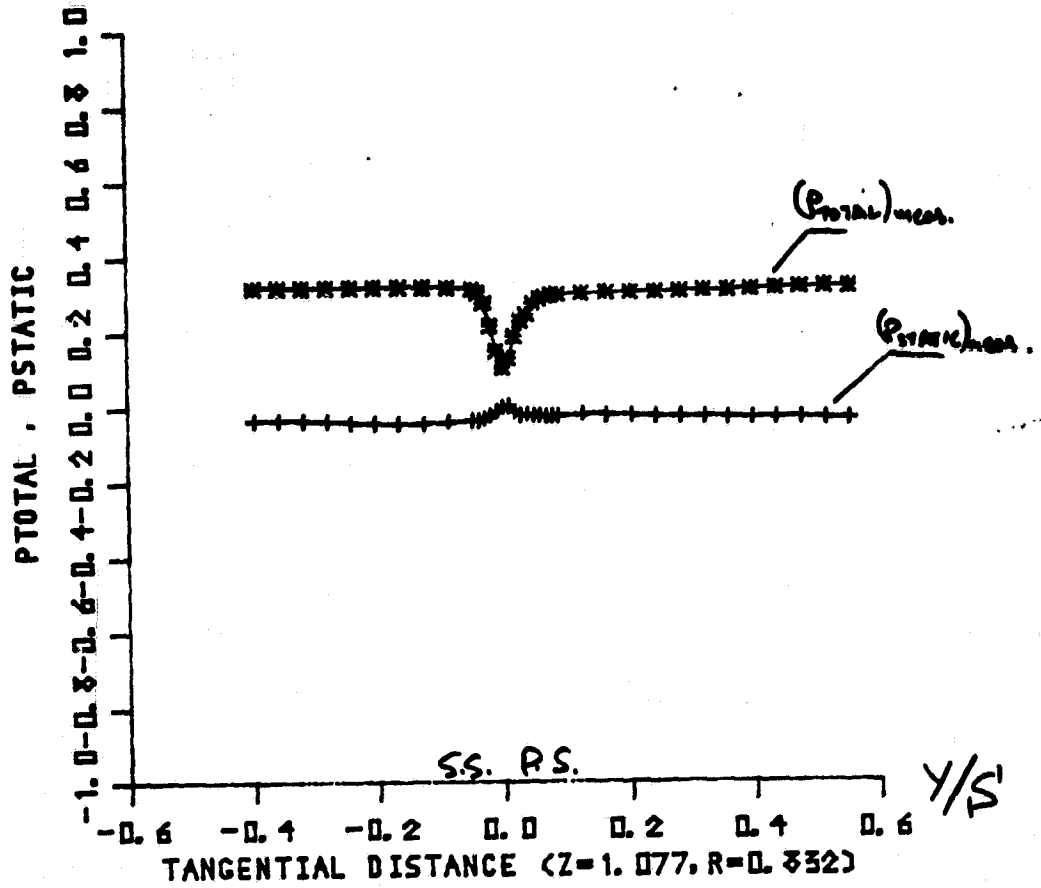


Figure 17. Stagnation (P_{TOTAL}) and static (P_{STATIC}) pressure profiles at $Z = 1.077$, $R = 0.832$

ORIGINAL PAGE IS
OF POOR QUALITY

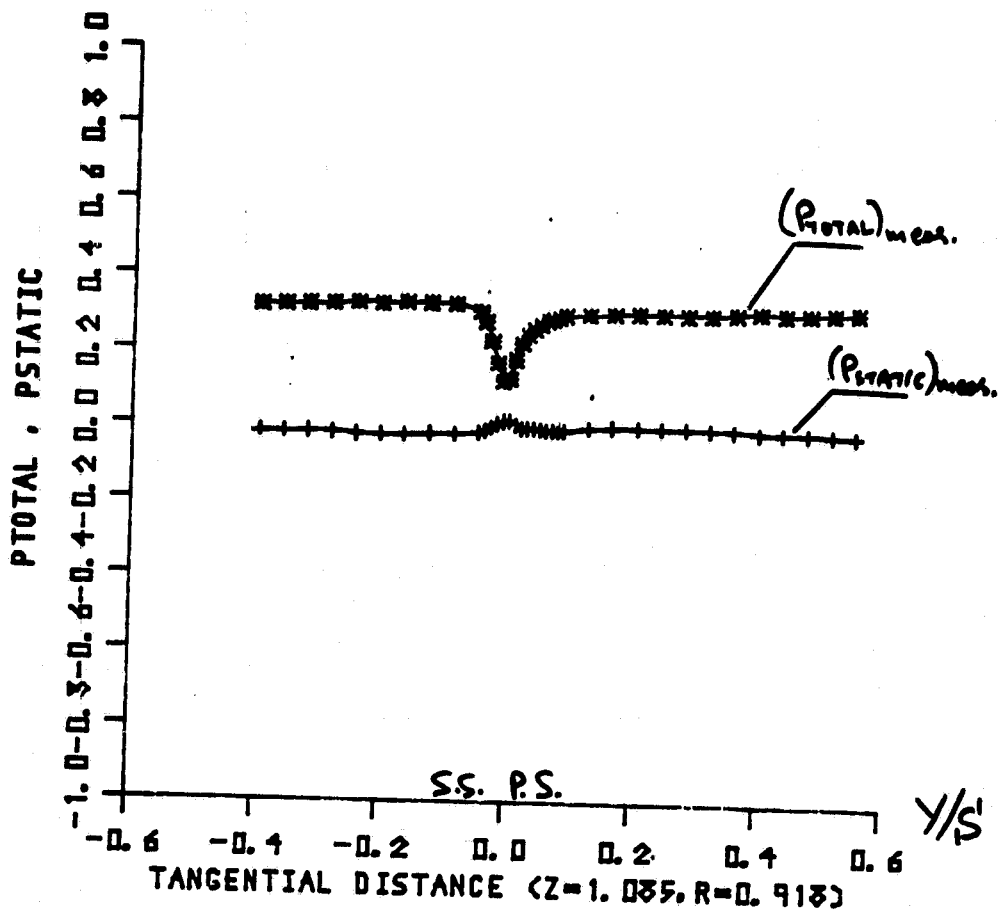


Figure 18. Stagnation (P_{TOTAL}) and static (P_{STATIC}) pressure profiles at $Z = 1.085$, $R = 0.918$